

**Dispersive readout with non-Markovian environments**H. Z. Shen <sup>1,2,\*</sup> Q. Wang,<sup>1</sup> and X. X. Yi<sup>1,2,†</sup><sup>1</sup>*Center for Quantum Sciences and School of Physics, Northeast Normal University, Changchun 130024, China*<sup>2</sup>*Center for Advanced Optoelectronic Functional Materials Research and Key Laboratory for UV Light-Emitting Materials and Technology of Ministry of Education, Northeast Normal University, Changchun 130024, China* (Received 1 June 2021; revised 6 December 2021; accepted 23 December 2021; published 10 February 2022)

We study the non-Markovian dispersive readout of a single-mode bosonic (SMB) quantum system coupled to the open cavity with two non-Markovian environments. Assuming that the SMB quantum system is initially prepared in a thermal equilibrium state, the susceptibility of the measured SMB quantum system to the cavity can be obtained by the nonequilibrium linear response theory, which provides the dispersive frequency shift of the cavity. We analytically derive the transmission and reflection of the cavity in the non-Markovian regime and discuss the non-Markovian dispersive readout of the SMB quantum system, which is in good agreement with that obtained by the Markovian approximation. We show that the effect of non-Markovian dynamics on the system's behavior leads to the decrease of the transmission and shifts of the frequency corresponding to the peak of the transmission in the dispersive regime compared with the Markovian case and the increase of the sum of the transmission and reflection due to the excitation backflowing induced by the couplings of the cavity and two non-Markovian environments, which could be applied to quantum secure direct communication with quantum memory. Finally, we generalize the readout theory to the periodically driven SMB quantum system based on the Floquet theory and quantum network, which contain all influences from the non-Markovian environments. The formalism presented in this paper opens an alternative field of possible applications in quantum information and quantum communication with non-Markovianity by manipulating the spectral densities of the environments.

DOI: [10.1103/PhysRevA.105.023707](https://doi.org/10.1103/PhysRevA.105.023707)**I. INTRODUCTION**

The storage, manipulation, and readout of the states of a quantum system are basic tasks in quantum information processing [1–3]. Dispersive measurement is implementable for the readout of quantum states of a qubit, when it strongly couples to a cavity [4–15]. The idea of the dispersive readout lies in the following. During the measurement, the qubit couples to the cavity off-resonantly, which results in the absence of energy exchange between them [16,17]. With the qubit-cavity system in the dispersive regime, frequency shifts occur for the cavity owing to the interaction with the qubit, which depend on the states of the qubit [15,18]. The shifts can be used to infer the quantum states. To do this, one can monitor the phase quadrature of the transmitted or the reflected radiation [15,19]. Alternatively, one measures the amplitude of the transmitted signal. Theoretically, the frequency shifts can be observed in the qubit-cavity Hamiltonian after a transformation to the dispersive frame [15], which is usually performed within the rotating-wave approximation (RWA).

With technological advancement, the dispersive readout has been applied to various solid-state systems, including the ac-driven quantum system [20,21], spin ensembles [22], quantum circuits [23–25], hybrid superconductor-semiconductor system [26], microwave resonator [27], cavity-coupled atom

[28,29], periodically driven quantum systems [30], Majorana fermions in a cavity [31], weakly coupled hybrid system [32], qubit readout [33], solid-state spin sensor [34], room-temperature spin qubits [35], and multilevel systems within the RWA [36,37]. Furthermore, the dispersive readout has been extended to the ultrastrong-coupling regime [21,38,39]. Indeed, strong- [14,40–43], ultrastrong- [44–47], and even deep-strong-coupling [48] regimes have been reached in circuit quantum electrodynamics (QED) systems, but they are still difficult to achieve for some other systems such as a single electron spin coupled to a cavity, which still remains in the weak-coupling regimes [5,6]. Experimental progress also has motivated several generalizations such as the treatment beyond the RWA [20,21,39,45,49]. Furthermore, the use of dispersive measurement techniques has allowed photon-number measurement [50–52] in cavity QED, which has been applied to mechanical resonators [53] coupled to both optical [54] and microwave cavities [55], the measurement of individual [56,57], and coupled superconducting qubits in circuit QED [58].

In recent years, with the rapid development of quantum information technology [1,59], the role played by the open quantum systems [60,61] has become more and more important. Generally speaking, all realistic quantum systems are open due to the unavoidable coupling with the environment [62–65]. The Markovian approximation for open systems [60,61] is only valid when the coupling between the system and environment is weak and the characteristic times of the bath are sufficiently smaller than those of the

\*Corresponding author: shenhz458@nenu.edu.cn

†Corresponding author: yixx@nenu.edu.cn

quantum system under study. Otherwise we should consider the effect of non-Markovian dynamics on the system's behavior, which occurs in many quantum systems including coupled cavities [66], optical fibers [67,68], trapped ions in colored noises [69–71], photonic crystals [72,73], and cavities coupled to waveguides [74–81]. The non-Markovian process proves to be useful in quantum information processing including quantum state engineering, quantum control, and quantum channel capacity [65,82–85]. Non-Markovianity can be characterized by the information flow between the system and its environment [86–92], which leads to different measures of non-Markovianity [93–98]. Thus the motivation of this paper is to determine the effect of non-Markovianity on the dispersive readout so that we can understand the fundamental physical origins of the non-Markovianity as well as the dispersive readout. These motivate us to explore the theory of dispersive readout in the non-Markovian regime.

In this paper we develop the theory of dispersive readout in a single-mode bosonic (SMB) quantum system coupled to the cavity by taking the effect of non-Markovian dynamics on the system's behavior into account. For this purpose, first the exact non-Markovian input-output relation is derived and then the susceptibility of the SMB quantum system to the cavity field is obtained with nonequilibrium linear response theory. The dispersive frequency shift of the cavity is also provided in terms of the SMB quantum system susceptibility, which can be probed experimentally by measuring the transmission spectrum of the cavity. We apply this theory to the time-independent system subjected to the non-Markovian environments and then find that the transmission spectrum changes from the non-Markovian to Markovian regimes by tuning the spectral densities of the environments. The non-Markovianity decreases the amplitude of transmission and shifts the frequency corresponding to the peak of the transmission compared with the Markovian case but increases the sum of the transmission and reflection in the dispersive regime. The non-Markovian dispersive readouts of the periodically driven SMB quantum system and quantum network are investigated when their susceptibility is derived based on the Floquet theory and quantum transmission line, which contains all influences from the non-Markovian environments. Finally, we demonstrate the feasibility of the theoretical scheme, indicating that the present scheme can be realized in experiments in the near future.

The remainder of this paper is organized as follows. We introduce the system-cavity model and Hamiltonian in Sec. II. In Sec. III the exact non-Markovian input-output relation is derived, which returns to the Markovian input-output relation in the Markovian limit. In Sec. IV the relation between the cavity transmission and the susceptibility of the SMB quantum system is given by the linear response theory and input-output relations in both Markovian and non-Markovian cases. The readout theory is applied to a time-independent multilevel system with a focus on the non-Markovian corrections in Sec. V. Section VI is devoted to the generalization to the periodically driven SMB quantum system. In Sec. VII we discuss the non-Markovian dispersive readout for a quantum network. We present a discussion of the experimental implementation of this scheme in Sec. VIII. We discuss and summarize our results in Sec. IX.

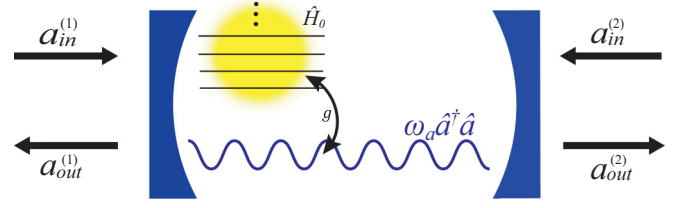


FIG. 1. Schematic of the proposed setup for the dispersive readout of the hybrid quantum system which consists of a SMB quantum system ( $\hat{H}_0 = \omega_c \hat{c}^\dagger \hat{c}$ ) and an open cavity with coupling constant  $g$ . The cavity couples to the input and output modes of two non-Markovian environments. Here  $a_{in}^{(v)}$  and  $a_{out}^{(v)}$  ( $v = 1, 2$ ) are the input and output-field operators. The input field incident from the right cavity mirror  $a_{in}^{(2)}$  is in the vacuum state and does not contribute to the average output fields.

## II. MODEL HAMILTONIAN

To present the general model to realize the dispersive readout in non-Markovian regimes, we consider here that a hybrid quantum system consists of a SMB quantum system and the cavity interacting with two non-Markovian environments, which is sketched in Fig. 1. The total system is governed by the Hamiltonian (setting  $\hbar = 1$ )

$$\hat{H} = \hat{H}_S + \hat{H}_I, \quad (1)$$

with

$$\begin{aligned} \hat{H}_S &= \omega_a \hat{a}^\dagger \hat{a} + g(\hat{c} + \hat{c}^\dagger)(\hat{a} + \hat{a}^\dagger) + \omega_c \hat{c}^\dagger \hat{c}, \\ \hat{H}_I &= \sum_k \omega_k \hat{b}_k^\dagger \hat{b}_k + \sum_k (g_k \hat{a} \hat{b}_k^\dagger + g_k^* \hat{a}^\dagger \hat{b}_k) \\ &\quad + \sum_k \Omega_k \hat{d}_k^\dagger \hat{d}_k + \sum_k (G_k \hat{a} \hat{d}_k^\dagger + G_k^* \hat{a}^\dagger \hat{d}_k), \end{aligned} \quad (2)$$

where  $\hat{a}^\dagger$  ( $\hat{a}$ ) is the creation (annihilation) operator of the cavity mode with frequency  $\omega_a$ ,  $\hat{c}^\dagger$  ( $\hat{c}$ ) is the creation (annihilation) operator of the bosonic mode with frequency  $\omega_c$ , and  $g$  is the coupling strength between the bosonic system and the cavity. The cavity couples to the  $k$ th mode (eigenfrequencies  $\omega_k$  and  $\Omega_k$ ) of the non-Markovian environments, which are modeled as collections of infinite modes via the creation (annihilation) operators  $\hat{b}_k^\dagger$  ( $\hat{b}_k$ ) and  $\hat{d}_k^\dagger$  ( $\hat{d}_k$ ). The parameters  $g_k$  and  $G_k$  are coupling coefficients between the two environments and the cavity, respectively.

Due to the coupling strength  $g$  between the bosonic system and the cavity, the cavity acts on the SMB quantum system, while it experiences a backaction that shifts the cavity frequency. This frequency shift allows one to infer the information about the bosonic system inside the cavity by driving the cavity with a laser and monitoring the changes of the cavity transmission resulting from the coupling between the SMB quantum system and the cavity.

## III. EXACT NON-MARKOVIAN INPUT-OUTPUT RELATIONS

We here analytically derive the exact non-Markovian input-output relation, which contains all the influences of the environments on the SMB quantum system. To treat the SMB

quantum system and the cavity as a hybrid quantum system, we move to the Heisenberg picture and use the Heisenberg equations for operators of the hybrid system. This treatment enables the calculation of the output fields at the ports of the cavity, given the input fields [36,37,99,100]. Generally in experiments, the cavity is probed by driving it with the input field and detecting the transmitted field.

In the Heisenberg picture, all operators including the cavity field, SMB quantum system, and environments are given by  $\hat{a}(t) = U^\dagger(t)\hat{a}U(t)$ ,  $\hat{c}(t) = U^\dagger(t)\hat{c}U(t)$ ,  $\hat{b}_k(t) = U^\dagger(t)\hat{b}_kU(t)$ , and  $\hat{d}_k(t) = U^\dagger(t)\hat{d}_kU(t)$ , where  $U(t) = \exp(-i\hat{H}t)$ , with  $\hat{H}$  given by Eq. (1). The time evolutions of the cavity and environment annihilation operators satisfy Heisenberg equation as follows:

$$\frac{d}{dt}\hat{a}(t) = -i[\hat{a}(t), \hat{H}(t)] = -i\omega_a\hat{a}(t) - ig[\hat{c}(t) + \hat{c}^\dagger(t)] - i\sum_k g_k^*\hat{b}_k(t) - i\sum_k G_k^*\hat{d}_k(t), \quad (3)$$

$$\frac{d}{dt}\hat{b}_k(t) = -i\omega_k\hat{b}_k(t) - ig_k\hat{a}(t), \quad (4)$$

$$\frac{d}{dt}\hat{d}_k(t) = -i\Omega_k\hat{d}_k(t) - iG_k\hat{a}(t). \quad (5)$$

Through simple calculations solving Eqs. (4) and (5), we obtain the formal solutions of the environment operators for  $0 \leq t$ , i.e.,

$$\begin{aligned} \hat{b}_k(t) &= \hat{b}_k(0)e^{-i\omega_k t} - ig_k \int_0^t d\tau \hat{a}(\tau)e^{-i\omega_k(t-\tau)}, \\ \hat{d}_k(t) &= \hat{d}_k(0)e^{-i\Omega_k t} - iG_k \int_0^t d\tau \hat{a}(\tau)e^{-i\Omega_k(t-\tau)}. \end{aligned} \quad (6)$$

The first terms on the right-hand sides of Eqs. (6) represent the freely propagating parts of the environment fields and the second terms describe the influences of the cavity. Substituting Eq. (6) into Eq. (3) for the cavity annihilation operator, we can obtain an integro-differential equation

$$\begin{aligned} \frac{d}{dt}\hat{a}(t) &= -i\omega_a\hat{a}(t) - ig[\hat{c}(t) + \hat{c}^\dagger(t)] - \hat{K}_1^\dagger(t) - \hat{K}_2^\dagger(t) \\ &\quad - \int_0^t d\tau \hat{a}(\tau)f_1(t-\tau) - \int_0^t d\tau \hat{a}(\tau)f_2(t-\tau), \end{aligned} \quad (7)$$

where the externally driven environment operators  $\hat{K}_1^\dagger(t) = i\sum_k g_k^*\hat{b}_k(0)e^{-i\omega_k t} = \int_{-\infty}^\infty d\tau \kappa_1^*(t-\tau)a_{\text{in}}^{(1)}(\tau)$  and  $\hat{K}_2^\dagger(t) = i\sum_k G_k^*\hat{d}_k(0)e^{-i\Omega_k t} = \int_{-\infty}^\infty d\tau \kappa_2^*(t-\tau)a_{\text{in}}^{(2)}(\tau)$ . The cavity couples to the incoming and outgoing modes of environments at both ends; thus we define here the input-field operators as  $a_{\text{in}}^{(1)}(t) = \frac{1}{\sqrt{2\pi}}\sum_k e^{-i\omega_k t}\hat{b}_k(0)$  and  $a_{\text{in}}^{(2)}(t) = \frac{-1}{\sqrt{2\pi}}\sum_k e^{-i\Omega_k t}\hat{d}_k(0)$  and the impulse response functions are  $\kappa_1(t) = \frac{-i}{\sqrt{2\pi}}\sum_k e^{i\omega_k t}g_k$  and  $\kappa_2(t) = \frac{i}{\sqrt{2\pi}}\sum_k e^{i\Omega_k t}G_k$ , or in the continuum

$$\begin{aligned} \kappa_1(t-\tau) &= \frac{-i}{\sqrt{2\pi}} \int e^{i\omega(t-\tau)}g(\omega)d\omega, \\ \kappa_2(t-\tau) &= \frac{i}{\sqrt{2\pi}} \int e^{i\omega(t-\tau)}G(\omega)d\omega, \end{aligned} \quad (8)$$

where we have made the replacements  $g_k \rightarrow g(\omega)$  and  $G_k \rightarrow G(\omega)$ . The correlation functions are given by

$$\begin{aligned} f_1(t) &= \sum_k |g_k|^2 e^{-i\omega_k t} = \int J_1(\omega)e^{-i\omega t}d\omega, \\ f_2(t) &= \sum_k |G_k|^2 e^{-i\Omega_k t} = \int J_2(\omega)e^{-i\omega t}d\omega, \end{aligned} \quad (9)$$

where  $J_1(\omega) = \sum_k |g_k|^2 \delta(\omega - \omega_k)$  and  $J_2(\omega) = \sum_k |G_k|^2 \delta(\omega - \Omega_k)$  represent the spectral densities of the two environments and  $f_1(t)$  and  $f_2(t)$  denote the memory functions of two environments, which describe the non-Markovian fluctuation-dissipation relationship of the environments.

In a similar manner, we obtain the formal solutions of the environment operators for  $t_1 \geq t$ , i.e.,

$$\hat{b}_k(t) = \hat{b}_k(t_1)e^{-i\omega_k(t-t_1)} + ig_k \int_{t_1}^t d\tau \hat{a}(\tau)e^{-i\omega_k(t-\tau)}, \quad (10)$$

$$\hat{d}_k(t) = \hat{d}_k(t_1)e^{-i\Omega_k(t-t_1)} + iG_k \int_{t_1}^t d\tau \hat{a}(\tau)e^{-i\Omega_k(t-\tau)}.$$

Similarly, we can obtain another integro-differential equation

$$\begin{aligned} \frac{d}{dt}\hat{a}(t) &= -i\omega_a\hat{a}(t) - ig[\hat{c}(t) + \hat{c}^\dagger(t)] - \hat{K}'_1(t) - \hat{K}'_2(t) \\ &\quad + \int_{t_1}^t d\tau \hat{a}(\tau)f_1(t-\tau) + \int_{t_1}^t d\tau \hat{a}(\tau)f_2(t-\tau), \end{aligned} \quad (11)$$

where we have defined the output-field operators and the externally driven environment operators as  $a_{\text{out}}^{(1)}(t) = \frac{1}{\sqrt{2\pi}}\sum_k e^{-i\omega_k(t-t_1)}\hat{b}_k(t_1)$  and  $a_{\text{out}}^{(2)}(t) = \frac{-1}{\sqrt{2\pi}}\sum_k e^{-i\Omega_k(t-t_1)}\hat{d}_k(t_1)$ , and  $\hat{K}'_1(t) = i\sum_k g_k^*\hat{b}_k(t_1)e^{-i\omega_k(t-t_1)} = \int_{-\infty}^\infty d\tau \kappa_1^*(t-\tau)a_{\text{out}}^{(1)}(\tau)$  and  $\hat{K}'_2(t) = i\sum_k G_k^*\hat{d}_k(t_1)e^{-i\Omega_k(t-t_1)} = \int_{-\infty}^\infty d\tau \kappa_2^*(t-\tau)a_{\text{out}}^{(2)}(\tau)$ , respectively.

By comparing Eq. (7) with Eq. (11), or summing of  $k$  to Eqs. (6) and (10), the input and output fields are connected by the non-Markovian input-output relation [101,102] for the cavity mirror  $\nu$  ( $\nu = 1, 2$ ) (setting  $t_1 \rightarrow t$ ),

$$a_{\text{out}}^{(\nu)}(t) - a_{\text{in}}^{(\nu)}(t) = \int_0^t d\tau \kappa_\nu(t-\tau)\hat{a}(\tau), \quad (12)$$

where the concrete form of  $\kappa_\nu(t-\tau)$  is given by Eq. (8). In the case of the Fabry-Pérot cavity [81], the spectral response functions can be defined by

$$\begin{aligned} g(\omega) &= \sqrt{\frac{\Gamma_1}{2\pi}} \frac{\lambda_1}{\lambda_1 - i\omega}, \\ G(\omega) &= \sqrt{\frac{\Gamma_2}{2\pi}} \frac{\lambda_2}{\lambda_2 - i\omega}, \end{aligned} \quad (13)$$

where  $\lambda_\nu$  ( $\nu = 1, 2$ ) is the environmental spectrum width and  $\Gamma_\nu$  is the cavity decay rate through the input and output ports. Thus the effective spectral density of the environments is [60,102–106]

$$J_\nu(\omega) = \frac{\Gamma_\nu}{2\pi} \frac{\lambda_\nu^2}{\lambda_\nu^2 + \omega^2}, \quad (14)$$

which corresponds to the Lorentzian spectral density. Specifically, the parameter  $\lambda_\nu$  is inversely proportional to the

environmental correlation time. With Eqs. (13) and (14), we obtain  $\kappa_1(\tau - t) = -i\sqrt{\Gamma_1}\lambda_1 e^{-\lambda_1(t-\tau)}\theta(t - \tau)$ ,  $\kappa_2(\tau - t) = i\sqrt{\Gamma_2}\lambda_2 e^{-\lambda_2(t-\tau)}\theta(t - \tau)$ ,  $f_1(t - \tau) = \frac{1}{2}\Gamma_1\lambda_1 e^{-\lambda_1|t-\tau|}$ , and  $f_2(t - \tau) = \frac{1}{2}\Gamma_2\lambda_2 e^{-\lambda_2|t-\tau|}$ , which represents a Gaussian Ornstein-Uhlenbeck process [107–109], where  $\theta(t - t')$  is the unit step function,  $\theta(t - t') = 1$  for  $t \geq t'$  otherwise  $\theta(t - t') = 0$ . When  $\lambda_v$  tends to infinity, the environment becomes memoryless. That is to say, in the wideband limit (i.e.,  $\lambda_v \rightarrow \infty$ ), the spectral density approximately takes  $J_v(\omega) \rightarrow \frac{\Gamma_v}{2\pi}$  or, equivalently,  $g(\omega) \rightarrow \sqrt{\frac{\Gamma_1}{2\pi}}$  and  $G(\omega) \rightarrow \sqrt{\frac{\Gamma_2}{2\pi}}$ . This describes the case in the Markovian limit. Then, according to Eqs. (8) and (9), we have  $f_v(t) = \Gamma_v\delta(t)$ ,  $\kappa_1(t) = -i\sqrt{\Gamma_1}\delta(t)$ , and  $\kappa_2(t) = i\sqrt{\Gamma_2}\delta(t)$ . Substituting these results into Eq. (12), we can obtain the Markovian input-output relation

$$\begin{aligned} a_{\text{out}}^{(1)}(t) - a_{\text{in}}^{(1)}(t) &= -i\sqrt{\Gamma_1}\hat{a}(t), \\ a_{\text{out}}^{(2)}(t) - a_{\text{in}}^{(2)}(t) &= i\sqrt{\Gamma_2}\hat{a}(t), \end{aligned} \quad (15)$$

where we show that the Markovian input-output relation given by Eqs. (15) is equivalent to that defined in Refs. [63,110,111] and can return to the result of Refs. [63,110,111] by the replacements  $g_k \rightarrow ig_k$  [ $g(\omega) \rightarrow ig(\omega)$ ] and  $G_k \rightarrow iG_k$  [ $G(\omega) \rightarrow iG(\omega)$ ] in Eqs. (2), (8), and (15).

#### IV. LINEAR RESPONSE THEORY

The response of the cavity to a probe field can be determined using the input-output theory, and the measurements of the cavity response provide useful information about the SMB quantum system embedded in the cavity. Both the amplitude and phase of the transmitted signal provide useful information about the SMB quantum system. For brevity, we restrict our discussion to the cavity amplitude response. In this section, by expressing the coupling operator  $\hat{O}(t) \equiv \hat{c}(t) + \hat{c}^\dagger(t)$  in terms of  $\hat{a}(t)$  to analytically solve Eq. (7), together with the non-Markovian input-output relation, we can obtain the transmission and reflection of the cavity.

Since we are not interested in quantum fluctuations of the cavity field, we consider Eq. (7) in its classical limit as an equation of motion for the expectation value  $a(t) \equiv \langle \hat{a}(t) \rangle$ . To obtain the expectation value of  $\hat{O}(t)$ , we assume that in the absence of the cavity, the SMB quantum system is described by a density matrix  $\rho_0(t) = U(t)\rho_0(0)U^\dagger(t)$ . Its dynamics is determined by the Liouville–von Neumann equation  $\dot{\rho}_0(t) = -i[\hat{H}_0, \rho_0(t)] \equiv -i\hat{L}_0(t)\rho_0(t)$ , with the Liouvillian  $\hat{L}_0(t)$ . Due to the interaction with the cavity, the SMB quantum system experiences an additional driving from the cavity. In Eq. (2) with  $\hat{a}$  and  $\hat{a}^\dagger$  replaced by classical amplitudes, the corresponding Hamiltonian becomes  $\hat{H}_{\text{ex}}(t) = \hat{O}F(t)$ , with  $F(t) = g[a(t) + a^*(t)]$ . When in the presence of the cavity, the dynamics of the SMB quantum system becomes

$$\dot{\rho}_{\text{ex}}(t) = -i\hat{L}_0(t)\rho_{\text{ex}}(t) - i\hat{L}_{\text{ex}}(t)\rho_0(t), \quad (16)$$

whose detailed derivation can be found in Appendix A. The solution of Eq. (16) is given by

$$\rho_{\text{ex}}(t) = -i \int_0^t P(t, t')\hat{L}_{\text{ex}}(t')\rho_0(t')dt', \quad (17)$$

where  $\hat{L}_{\text{ex}}(t')\rho_0(t') = [\hat{H}_{\text{ex}}(t'), \rho_0(t')]$  and  $P(t, t') = \mathcal{T} \exp[-i \int_{t'}^t \hat{L}_0(\tau)d\tau]$  is the propagator of  $\hat{L}_0(t)$  with the time-ordering operator  $\mathcal{T}$ . Then the change rate of the expectation value for the operator  $\hat{O}(t) = e^{i\hat{H}_0 t} \hat{O} e^{-i\hat{H}_0 t}$  reads

$$O(t) \equiv \text{Tr}\{\hat{O}\rho_{\text{ex}}(t)\} = \int_0^t dt' \chi(t, t')g[a(t') + a^*(t')], \quad (18)$$

where the susceptibility

$$\begin{aligned} \chi(t, t') &= -i \text{Tr}\{\hat{O}P(t, t')[\hat{O}, \rho_0(t')]\}\theta(t - t') \\ &= -i \text{Tr}\{[\hat{O}(t), \hat{O}(t')]\rho_0\}\theta(t - t'). \end{aligned} \quad (19)$$

Making a modified Laplace transformation [112–114]  $\eta(\omega) = \int_0^\infty e^{i\omega t} \eta(t)dt$  to Eq. (7), where  $e^{i\omega t} \rightarrow e^{i\omega t - \epsilon t}$  with  $\epsilon \rightarrow 0^+$  makes  $\eta(\omega)$  to converge to a finite value, we find the cavity equation

$$\begin{aligned} -i\omega a(\omega) &= -i\omega_a a(\omega) - a(\omega)f_1(\omega) - \tilde{\kappa}_1(\omega)[a_{\text{in}}^{(1)}(\omega) - a_{\text{in}}^{(1)}(i\lambda_1)] \\ &\quad - igO(\omega) - a(\omega)f_2(\omega) - \tilde{\kappa}_2(\omega)[a_{\text{in}}^{(2)}(\omega) - a_{\text{in}}^{(2)}(i\lambda_1)], \end{aligned} \quad (20)$$

with  $\tilde{\kappa}_v(\omega) = \int_{-\infty}^0 \kappa_v^*(t')e^{i\omega t'} dt'$ ,  $a_{\text{in}}^{(v)}(\omega) = \int_0^\infty a_{\text{in}}^{(v)}(t')e^{i\omega t'} dt'$ , and  $f_v(\omega) = \int_0^\infty f_v(t')e^{i\omega t'} dt'$ . For the undriven system, the susceptibility depends only on the time difference  $t - t'$  such that the integration in Eq. (18) is a convolution and in frequency space reads  $O(\omega) = g\chi(\omega)[a(\omega) + a^*(-\omega)]$ , which leads to Eq. (20) becoming

$$\begin{aligned} &[-i\omega + i\omega_a + f_1(\omega) + f_2(\omega)]a(\omega) \\ &\quad + ig^2\chi(\omega)[a(\omega) + a^*(-\omega)] \\ &= -\tilde{\kappa}_1(\omega)[a_{\text{in}}^{(1)}(\omega) - a_{\text{in}}^{(1)}(i\lambda_1)] \\ &\quad - \tilde{\kappa}_2(\omega)[a_{\text{in}}^{(2)}(\omega) - a_{\text{in}}^{(2)}(i\lambda_1)]. \end{aligned} \quad (21)$$

For a high-finesse cavity, small detuning  $\omega - \omega_a$ , and sufficiently small coupling  $g$  such that

$$|\tilde{\kappa}_1(\omega)|^2, |\tilde{\kappa}_2(\omega)|^2, |\omega - \omega_a|, |g^2\chi(\omega)| \ll \omega_a, \quad (22)$$

the impact of  $a^*(-\omega)$  is negligible (for the reasons, see Appendix B), which means that the SMB quantum system response is  $O(\omega) = g\chi(\omega)a(\omega)$ . Then the solution of Eq. (21) together with the non-Markovian input-output relation given by Eq. (12) yields the cavity transmission  $\tilde{t}_c = a_{\text{out}}^{(2)}(\omega)/a_{\text{in}}^{(1)}(\omega) = t_c + \varphi_1$  with  $\varphi_1 = -\phi(\lambda_1, \omega)t_c$  and  $\phi(\lambda_1, \omega) = a_{\text{in}}^{(1)}(i\lambda_1)/a_{\text{in}}^{(1)}(\omega)$ , and reflection  $\tilde{r}_c = a_{\text{out}}^{(1)}(\omega)/a_{\text{in}}^{(1)}(\omega) = r_c + \varphi_2$  with  $\varphi_2 = -\phi(\lambda_1, \omega)r_c$  amplitudes at frequency  $\omega$ , where

$$\begin{aligned} t_c &= \frac{i\tilde{\kappa}_1(\omega)\kappa_2(-\omega)}{\omega_a - \omega - i[f_1(\omega) + f_2(\omega)] + g^2\chi(\omega)}, \\ r_c &= \frac{i\tilde{\kappa}_1(\omega)\kappa_1(-\omega)}{\omega_a - \omega - i[f_1(\omega) + f_2(\omega)] + g^2\chi(\omega)} + 1, \end{aligned} \quad (23)$$

where  $\kappa_v(\omega) = \int_{-\infty}^0 \kappa_v(t')e^{i\omega t'} dt'$ , and we have assumed that  $a_{\text{in}}^{(2)}(\omega)$  is in the vacuum state. Their dependence on  $\chi(\omega)$  allows us to obtain the information about the SMB quantum system by probing the reflection  $|r_c|^2$  or transmission  $|t_c|^2$ .

We find that  $\varphi_1 = -\phi(\lambda_1, \omega)t_c$  and  $\varphi_2 = -\phi(\lambda_1, \omega)r_c$  are induced by non-Markovian effect and have no Markovian counterparts, which are inhomogeneous terms depending on the specific forms of the input field  $a_{\text{in}}^{(1)}(t)$ . In Markovian approximation,  $\phi(\lambda_1, \omega)$  tends to zero for  $\lambda_1 \rightarrow \infty$ . In order to see the effect of this inhomogeneous term, we now assume that the input field  $a_{\text{in}}^{(1)}(t)$  has two concrete forms as follows: damped oscillation  $a_{\text{in}}^{(1)}(t) = a_1 e^{-\gamma t} \sin(b_1 t^2)$  and Gaussian profile  $a_{\text{in}}^{(1)}(t) = a_1 e^{-\gamma t^2} \cos(b_1 t)$  for  $\gamma > 0$  and  $b_1 > 0$ , which respectively correspond to  $\phi(\lambda_1, \omega) = \{\cos[\frac{(\gamma+\lambda)^2}{4b_1}][1 - 2fc(\frac{\gamma+\lambda}{\sqrt{2\pi b_1}})] + [1 - 2fs(\frac{\gamma+\lambda}{\sqrt{2\pi b_1}})] \sin[\frac{(\gamma+\lambda)^2}{4b_1}]\} / \{\cos[\frac{(\gamma-i\omega)^2}{4b_1}][1 - 2fc(\frac{\gamma-i\omega}{\sqrt{2\pi b_1}})] + [1 - 2fs(\frac{\gamma-i\omega}{\sqrt{2\pi b_1}})] \sin[\frac{(\gamma-i\omega)^2}{4b_1}]\}$  and  $\phi(\lambda_1, \omega) = e^{\frac{\lambda^2 + \omega^2 + 2b_1(\omega - i\lambda)}{4\gamma}} \{i + e^{\frac{ib_1\lambda}{\gamma}} [i + \text{erfi}(\frac{b_1 - i\lambda}{2\sqrt{\gamma}})] - \text{erfi}(\frac{b_1 + i\lambda}{2\sqrt{\gamma}})\} / \{i + e^{\frac{b_1\omega}{\gamma}} [i + \text{erfi}(\frac{b_1 - \omega}{2\sqrt{\gamma}})] - \text{erfi}(\frac{b_1 + \omega}{2\sqrt{\gamma}})\}$ , where  $fc(z) = \int_0^z \cos(\pi t^2/2) dt$ ,  $fs(z) = \int_0^z \sin(\pi t^2/2) dt$ ,  $\text{erfi}(z) = \text{erf}(iz)/i$  with  $\text{erf}(z) = \frac{2}{\sqrt{\pi}} \int_0^z e^{-t^2} dt$ .

We show the inhomogeneous terms can not reveal the properties of the SMB quantum system to be tested. For two concrete input fields and given parameters, e.g.,  $\gamma = 0.001\omega_a$ ,  $b_1 = 0.003\omega_a$ , we can evaluate  $|\phi(\lambda_1, \omega)| \sim 10^{-3}$  for  $\lambda = 0.5\omega_a$  (non-Markovian regime), and  $|\phi(\lambda_1, \omega)| \sim 10^{-6}$  for  $\lambda = 5\omega_a$  (weak non-Markovian effect) at the interval  $\omega \in (0.9\omega_a, 1.2\omega_a)$  for the above two cases. This means that the inhomogeneous terms  $|\varphi_1|$  and  $|\varphi_2|$  are much smaller than the transmission  $|t_c|$  and reflection  $|r_c|$ , which therefore can be ignored for these parameters, and leads to  $\tilde{t}_c \sim t_c$  and  $\tilde{r}_c \sim r_c$  for two above input fields. Therefore, the influences of the inhomogeneous terms on the cavity transmission and reflection will be not considered for plotting later.

In addition, we also can redefine the cavity transmission with non-Markovian regimes as  $t_c = a_{\text{out}}^{(2)}(\omega)/[a_{\text{in}}^{(1)}(\omega) - a_{\text{in}}^{(1)}(i\lambda_1)] = \frac{i\tilde{\kappa}_1(\omega)\kappa_2(-\omega)}{\omega_a - \omega - i[f_1(\omega) + f_2(\omega)] + g^2\chi(\omega)}$  given by Eq. (23) which can reflect the properties of the SMB quantum system.

In the Markovian limit (i.e.,  $\lambda_v \rightarrow \infty$ ), we have  $\tilde{\kappa}_1(\omega) \rightarrow i\sqrt{\Gamma_1}$ ,  $\kappa_1(\omega) \rightarrow -i\sqrt{\Gamma_1}$ ,  $\kappa_2(\omega) \rightarrow i\sqrt{\Gamma_2}$ , and  $f_v(\omega) \rightarrow \Gamma_v/2$ . Substituting these results into Eq. (23), we can obtain the Markovian transmission and reflection amplitudes of the cavity [21]

$$\begin{aligned} t_{\text{cm}} &= \frac{-i\sqrt{\Gamma_1\Gamma_2}}{\omega_a - \omega - i\Gamma/2 + g^2\chi(\omega)}, \\ r_{\text{cm}} &= \frac{i\Gamma_1}{\omega_a - \omega - i\Gamma/2 + g^2\chi(\omega)} + 1, \end{aligned} \quad (24)$$

where the total cavity decay rate  $\Gamma \equiv \Gamma_1 + \Gamma_2$ . As compared to the absence of the bosonic system, the maximum of the transmission is shifted away from  $\omega = \omega_a$  by  $g^2\text{Re}\chi(\omega)$ .

## V. TIME-INDEPENDENT SINGLE-MODE BOSONIC SYSTEM

So far, many works start from the coupled quantum Langevin equations of the cavity and system, which are solved within the RWA to obtain the cavity response [36,37,115–117]. We consider the SMB quantum system ( $\hat{H}_0 = \omega_c \hat{c}^\dagger \hat{c}$ ) initially prepared in a thermal equilibrium state with the tem-

perature  $T$  as

$$\begin{aligned} \rho_0 &= \exp(-\hat{H}_0/\kappa_B T) / \text{Tr} \exp(-\hat{H}_0/\kappa_B T) \\ &= \sum_n p_n |n\rangle \langle n|, \end{aligned} \quad (25)$$

where the population  $p_n = \frac{(\hat{c}^\dagger \hat{c})^n}{(1 + (\hat{c}^\dagger \hat{c})^n)^{n+1}}$  ( $n = 0, 1, 2, \dots$ ) with  $\langle \hat{c}^\dagger \hat{c} \rangle = (e^{\hbar\omega_c/\kappa_B T} - 1)^{-1}$ . Here  $\kappa_B$  is the Boltzmann constant. The eigenequation is  $\hat{H}_0 |n\rangle = E_n |n\rangle$  with the eigenvalues  $E_n = \omega_c n$ . In this case, with Eq. (19), we can obtain [21]

$$\chi(\omega) = \sum_{m,n} \frac{(p_m - p_n) |O_{mn}|^2}{\omega + E_m - E_n + i\gamma_{mn}/2}, \quad (26)$$

where  $\gamma_{mn}$  denotes the decay rate introduced phenomenologically. Obviously,  $\text{Re}\chi(\omega)$  has peaks at  $\omega = E_n - E_m$ ; for resonant cavity input ( $\omega = \omega_a$ ), these peaks turn into dips in the transmission. As  $\chi(\omega)$  has to be calculated at  $\omega = \omega_a > 0$ , terms with  $E_m > E_n$  are off-resonant and smaller than the ones with interchanged indices. Consequently, we can restrict the summation to terms with  $m < n$  to obtain the RWA result for the cavity response [36], while Eq. (26) generalizes the result beyond the RWA and gives the non-RWA corrections [37,39].

The matrix element of the coupling operator satisfies  $O_{mn} = \langle m | \hat{O} | n \rangle = \langle m | \hat{c} + \hat{c}^\dagger | n \rangle = \sqrt{n} \delta_{m,n-1} + \sqrt{n+1} \delta_{m,n+1}$  and then  $|O_{mn}|^2 = n \delta_{m,n-1} + (n+1) \delta_{m,n+1}$ . Consequently, we can rewrite Eq. (26) as the sum of two summations

$$\begin{aligned} \chi(\omega) &= \sum_n \frac{(p_{n-1} - p_n)n}{\omega + E_{n-1} - E_n + i\gamma_{n-1,n}/2} \\ &+ \sum_n \frac{(p_{n+1} - p_n)(n+1)}{\omega + E_{n+1} - E_n + i\gamma_{n+1,n}/2}, \end{aligned} \quad (27)$$

which corresponds to the result beyond the rotating-wave approximation. By neglecting the second summation, we can obtain the RWA result (see Appendix C for more details). If  $\chi(\omega)$  is real, we can readily find  $|r_{\text{cm}}|^2 + |t_{\text{cm}}|^2 = 1$ , which reflects energy conservation. By contrast, in the case given by Eq. (26) or (27) at thermal equilibrium with the temperature  $T$ , we show that the sum of cavity transmission and reflection is less than one, i.e.,

$$|r_{\text{cm}}|^2 + |t_{\text{cm}}|^2 < 1, \quad (28)$$

since the imaginary part of susceptibility is less than zero in the whole parameter regime, i.e.,  $\text{Im}\chi(\omega) < 0$ , which implies energy transfers from the cavity to the SMB quantum system and the SMB quantum system dissipates energy with the decay rate  $\gamma_{mn}$ . The detailed derivation of Eq. (28) can be found in Appendix D. If one establishes some other mechanisms, for example, the SMB quantum system transfers energy to the cavity or the environmental photons flow back to the cavity such that  $|r_{\text{cm}}|^2 + |t_{\text{cm}}|^2$  might be greater than one in some parameter regimes. We show that the non-Markovian dispersive readout belongs to the latter, which will be discussed in Sec. VB.

### A. Dispersive readout in the Markovian case

We consider that both environments have Lorentzian spectra. In the Markovian limit ( $\lambda_v \rightarrow \infty$ ), we have derived the

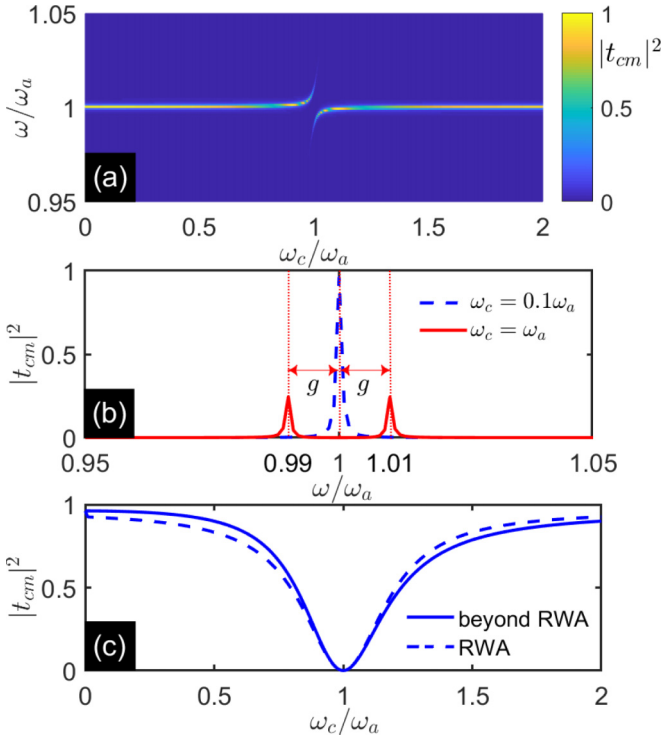


FIG. 2. (a) Cavity transmission spectra  $|t_{cm}|^2$  given by Eq. (24) as a function of  $\omega$  and/or  $\omega_c$  at zero temperature. (b) The blue dashed line (red solid line) represents  $|t_{cm}|^2$  as a function of  $\omega$  for  $\omega_c = 0.1\omega_a$  ( $\omega_c = \omega_a$ ). (c) The blue solid (dashed) line shows  $|t_{cm}|^2$  as a function of  $\omega_c$  in the beyond RWA (RWA) case with  $\omega = \omega_a$ . The cavity is symmetric ( $\Gamma_1 = \Gamma_2 = \Gamma/2$  with  $Q = 1000$ ) and the coupling  $g = 0.01\omega_a$ . The other parameter is  $\gamma_{mn} = 0.001\omega_c$ . Here and in other figures, all plotted quantities are dimensionless.

Markovian input-output relation given by Eq. (15) and the Markovian transmission and reflection amplitudes given by Eq. (24). Figure 2(a) shows the anticrossing between the cavity mode and the state of the SMB quantum system by depicting the calculated transmission of the cavity  $|t_{cm}|^2$  given by Eq. (24) as a function of the driving frequency  $\omega$  and the level splitting  $\omega_c$ . For this time-independent multilevel system, the level splitting occurs at  $\omega_c = E_{n+1} - E_n$ . When the driving frequency is near the cavity frequency, we can see the emergence of two peaks. The characteristic frequency splitting of the coupled modes gives the coupling rate of  $g = 0.01\omega_a$ , which is greater than the linewidth of both the cavity mode and the bosonic mode ( $\Gamma \equiv \omega_a/Q$  and  $\gamma_{mn} = 0.001\omega_c$ , respectively). This indicates that the strong-coupling regime  $g \gg \Gamma, \gamma_{mn}$  is achieved, which can be used to perform a quantum nondemolition measurement of the state of the bosonic system in the nonresonant (dispersive) limit, i.e.,  $g \ll |\omega_c - \omega_a|$ .

In Fig. 2(b) the vacuum Rabi splitting is readily observable from the red solid line when  $\omega_c = \omega_a$ . As indicated with the red arrows, the coupling strength  $g$  relates to the separation between the two symmetric peaks, which is also described as the vacuum Rabi frequency. The strong-coupling condition is defined as having a sufficiently large interaction such that two separated peaks are observable in the system response [36]. However, when the transition frequency is away from the

cavity frequency, the blue dashed line shows that the vacuum Rabi splitting disappears and a peak appears at  $\omega = \omega_a$ , which corresponds to the occurrence of the dispersive limit of the interaction. In this dispersive regime, i.e.,

$$g \ll |\omega_c - \omega_a|, \quad (29)$$

the probing of the cavity mode can be used to infer the property and state of the SMB quantum system with a backaction. Figure 2(c) demonstrates that when the cavity frequency is close to the transition frequency, the interaction between the bosonic system and the cavity results in a significantly reduced cavity transmission, while far from resonance, the cavity transmission is perfect. Actually, at zero temperature, the transition between the excited states remains dark, which can be explained by the vanishing populations  $p_n = 0$  ( $n > 0$ ). However, most of the population is in the ground state and correspondingly only the transition  $|0\rangle \rightarrow |1\rangle$  is excited and the corresponding transition frequency is in resonance with the cavity frequency, i.e.,  $E_1 - E_0 = \omega_c = \omega_a$ . Moreover, the non-RWA term has a significant effect on the shape of the dip, which may be relevant for quantitative comparisons between experiment and theory.

In the present case, we are dealing with the bosonic system at zero temperature, equivalently reducing to a two-level system. In the usual scenario of a two-level system coupled to an optical cavity, strong coupling results in light-matter hybridization, as evidenced in the observation of vacuum Rabi splitting and the corresponding anticrossing in the cavity transmission spectrum when the level transition frequency matches the cavity frequency. The two vacuum Rabi normal modes are separated by the vacuum Rabi frequency, and the linewidth of each mode reflects the average decoherence rate of light and matter [118].

Next we consider the effect of the temperature on the cavity transmission. In Fig. 3(a) we show the cavity transmission  $|t_{cm}|^2$  as a function of  $\omega_c$  and  $T$ . Figures 3(b) and 3(c) show the horizontal and vertical cuts of this plot at different values of  $\omega_c$  and  $T$ . From Fig. 3(b) we can see that when  $\omega_c = \omega_a$ , the interaction between the bosonic system and the cavity results in a significant reduction in the cavity transmission despite the temperatures. As the temperature increases, the population of the excited states  $p_n$  ( $n > 0$ ) increases and these states start contributing to the cavity response. The cavity response becomes weaker, which is visible in the reduced linewidth (width of the dip). The transition  $|n\rangle \rightarrow |n+1\rangle$  can be excited with  $E_{n+1} - E_n = \omega_c = \omega_a$ . We can also see that the quality of the RWA is expected to improve for higher temperature from Fig. 3(b). Similarly, from Fig. 3(c) we can find that  $|t_{cm}|^2 = 0$  when  $\omega_c = \omega_a$  and  $|t_{cm}|^2 \rightarrow 1$  when  $\omega_c$  is far from  $\omega_a$ . In the two cases, the temperature has almost no effect on the transmission, but influences the transmission when  $\omega_c$  is close to  $\omega_a$  ( $\omega_c = 0.9\omega_a$ ). It is worth noting that, starting from Fig. 3, the multilevel system is truncated into a finite level ( $n = 25$ ) in the numerical simulation, which makes no difference to the result with an infinite level.

We next show the cavity transmission plotted as a function of  $\omega$  and  $T$  in Fig. 4. We can see that the vacuum Rabi splitting (only the transition  $|0\rangle \rightarrow |1\rangle$ ) appears at zero temperature when the SMB quantum system is in resonance with the cavity, i.e.,  $\omega_c = \omega_a$ . However, there still exists the splitting

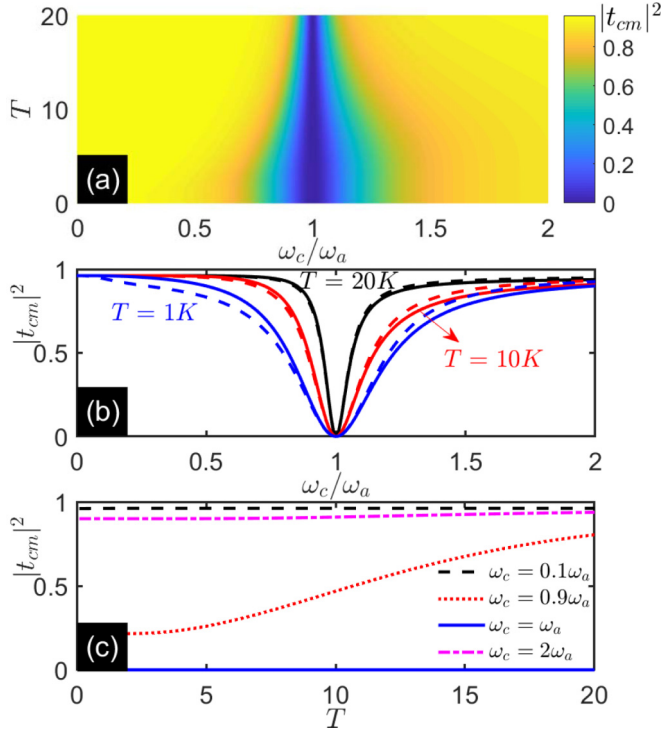


FIG. 3. (a) Cavity transmission spectra  $|t_{cm}|^2$  given by Eq. (24) as a function of  $\omega_c$  and/or the temperature  $T$ . (b) The solid (dashed) lines correspond to the beyond RWA (RWA) results representing  $|t_{cm}|^2$  as a function of  $\omega_c$  at different temperatures. (c) Lines show  $|t_{cm}|^2$  as a function of  $T$  for different  $\omega_c$ . The other parameters are the same as those in Fig. 2 but with  $\omega = \omega_a$ .

as the temperature increases, which originates from the transition  $|n\rangle \rightarrow |n+1\rangle$  with  $E_{n+1} - E_n = \omega_c = \omega_a$ . There are also two peaks for the finite temperature in Fig. 4(a), where the splitting between the two peaks decreases as the temperature increases. Therefore, it cannot be called vacuum Rabi splitting for the finite temperature, while for  $\omega_c = 0.1\omega_a$ , there is no

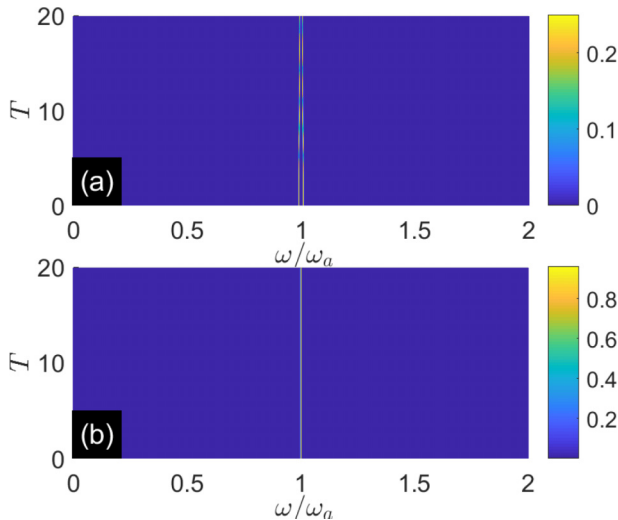


FIG. 4. Cavity transmission spectra  $|t_{cm}|^2$  given by Eq. (24) as a function of  $\omega$  and  $T$ , with (a)  $\omega_c = \omega_a$  and (b)  $\omega_c = 0.1\omega_a$ . The other parameters are the same as those in Fig. 2.

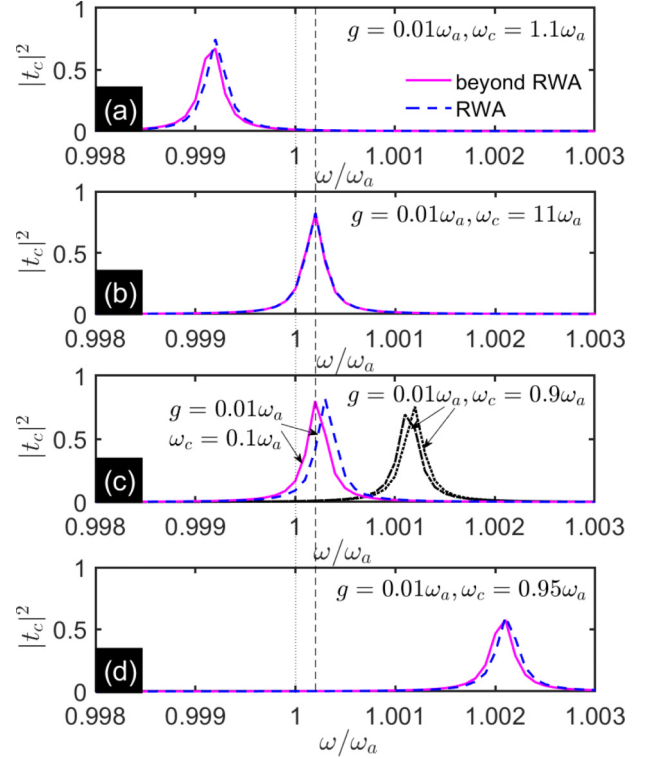


FIG. 5. Non-Markovian cavity transmission spectra  $|t_c|^2$  given by Eq. (23) as a function of  $\omega$  with different values of  $\omega_c$ : (a)  $\omega_c = 1.1\omega_a$ , (b)  $\omega_c = 11\omega_a$ , (c)  $\omega_c = 0.1\omega_a$ ,  $\omega_c = 0.9\omega_a$ , and (d)  $\omega_c = 0.95\omega_a$ . The magenta solid lines in all panels and the black dash-dotted line in (c) represent the beyond RWA results and the blue dashed lines in all panels and the black dotted line in (c) represent the RWA results. We choose the parameters  $\lambda_1 = \lambda_2 = 0.5\omega_a$  and  $g = 0.01\omega_a$ ; the other parameters are the same as those in Fig. 2.

Rabi splitting despite the temperatures, as shown in Fig. 4(b). Comparing the two panels, from the color coding we also can see that the amplitude of the transmission in Fig. 4(a) is much smaller than that in Fig. 4(b).

## B. Dispersive readout in the non-Markovian case

For open quantum systems, the Markovian approximation is only valid when the coupling between the quantum system and the environment is weak and the characteristic time of the environment is sufficiently shorter than that of the quantum system. The effect of the non-Markovian dynamics on the system's behavior should be taken into account when the coherent time (or environmental correlation time) is long.

As we know, the RWA needs to meet two conditions,

$$\begin{aligned} g &\ll \omega_c + \omega_a, \\ |\omega_c - \omega_a| &\ll \omega_c + \omega_a, \end{aligned} \quad (30)$$

which are derived in Appendix E. In general, the RWA does not work if we break one of the conditions, and the non-RWA (beyond RWA) results are not the same as the RWA results. From the magenta solid lines and the blue dashed lines in Figs. 5(a) and 5(d) given by Eq. (23), we can see that the beyond RWA results give the same dispersive frequency shift as the RWA results when both conditions of the RWA hold.

In these two cases, the coupling satisfies  $g < |\omega_a - \omega_c|$  but not  $g \ll |\omega_a - \omega_c|$ , which means the dispersive readout is less effective. However, from the magenta solid lines and the blue dashed lines in Figs. 5(b) and 5(c) it is easy to find that  $g \ll |\omega_a - \omega_c|$  holds but  $|\omega_c - \omega_a| \ll \omega_c + \omega_a$  breaks. In Fig. 5(b) the two results overlap precisely, which means that the dispersive readout is very effective with  $g = 0.01\omega_a \ll |\omega_a - \omega_c| = 10\omega_a$  even though the RWA is violated, while in Fig. 5(c) the frequency shift of the RWA result is different from the beyond RWA result when  $g = 0.01\omega_a \ll |\omega_a - \omega_c| = 0.9\omega_a$  and the RWA is violated. That is to say, the dispersive readout is effective but not better than that in Fig. 5(b); however, the readout beyond the RWA in Fig. 5(c) shows great agreement with the results in Fig. 5(b). From Figs. 5(c) and 5(d) we can see that the dispersive shift moves right as  $\omega_c/\omega_a$  changes from 0.1 to 0.95. Similarly, the dispersive shift moves left as  $\omega_c/\omega_a$  changes from 11 to 1.1, shown Figs. 5(b) and 5(a). In the next figure, we will choose the result beyond the RWA with the parameters  $g = 0.01\omega_a$  and  $\omega_c = 0.1\omega_a$  to show the effects of the non-Markovianity on the dispersive readout. From Fig. 5, in this dispersive regime, we show that the shift  $(\omega_M - \omega_a)$  between the frequency  $\omega_M$  corresponding to the peak value of the transmission and the bare cavity frequency induced by the effects of non-Markovian dynamics on the system's behavior can be obtained by the root  $\omega_M$  of

$$z(\omega)t_c^* + z^*(\omega)t_c = 0, \quad (31)$$

with

$$z(\omega) = \frac{[\omega_a + z_1(\omega) - \omega]\dot{z}_2(\omega) - z_2(\omega)[\dot{z}_1(\omega) - 1]}{[\dot{z}_1(\omega) - \omega + \omega_a]^2}, \quad (32)$$

which originates from the derivative of the transmission  $t_c$  given by Eq. (23) to the frequency, where  $z_1(\omega) = g^2\chi(\omega) - i[f_1(\omega) + f_2(\omega)]$ ,  $z_2(\omega) = i\tilde{\kappa}_1(\omega)\kappa_2(\omega)$ .

We next discuss the effects of the non-Markovianity on the dispersive readout with the Gaussian Ornstein-Uhlenbeck process. We restrict the discussion to rather low temperature, at which thermal excitations do not play a role. In the dispersive limit, the dispersive pull of the cavity frequency by the SMB quantum system can be used to entangle the state of the SMB quantum system with that of the photons transmitted or reflected by the cavity [15]. It is interesting to note that such entangled states may be used to couple the SMB quantum system in distant resonators and allow quantum communication [119]. From Fig. 6(a) we can see that the non-Markovian transmission  $|t_c|^2$  at  $\lambda_1 = \lambda_2 = 300\omega_a$  denoted by the black solid line overlaps precisely with the Markovian transmission  $|t_{cm}|^2$  denoted by the yellow diamond dashed line. As the two symmetric spectrum widths decrease, the dispersive pull of the cavity increases. It is easy to see that  $|t_c|^2$  also decreases with reduced linewidth for smaller spectrum widths (i.e.,  $\lambda_1 = \lambda_2 = 0.5\omega_a$ , corresponding to the case in the non-Markovian regime) compared to that with larger spectrum widths. Interestingly, the cavity transmission with asymmetric spectrum widths (i.e.,  $\lambda_1 \neq \lambda_2$ ) shows some different phenomena in Fig. 6(b). When  $\lambda_1 = 0.5\omega_a$  and  $\lambda_2 = 300\omega_a$ , corresponding to the case that one environment is Markovian but the other is non-Markovian, the cavity transmission shows a smaller amplitude and larger linewidth compared to the case with

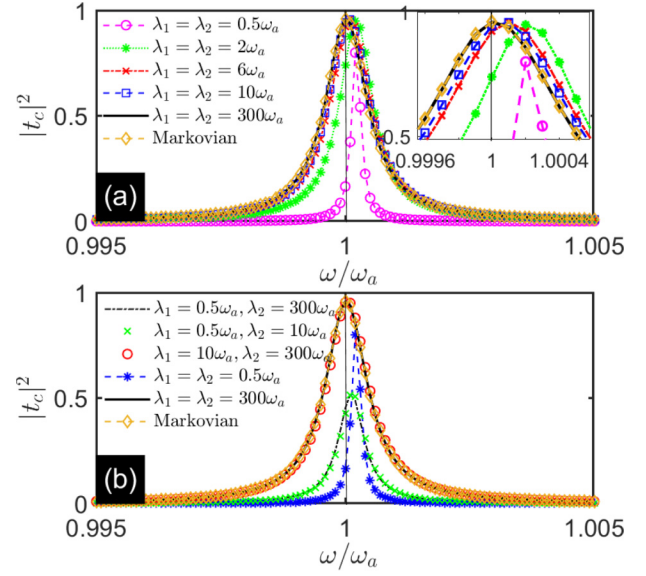


FIG. 6. Non-Markovian cavity transmission spectra  $|t_c|^2$  given by Eq. (23) as a function of  $\omega$ , with (a) a symmetric spectrum width ( $\lambda_1 = \lambda_2$ ) and (b) an asymmetric spectrum width ( $\lambda_1 \neq \lambda_2$ ). The inset is an enlargement of the region in (a). Note that as the environmental spectrum width  $\lambda_v$  increases, the non-Markovian readout effect gradually shifts the frequency corresponding to the peak of the transmission in the dispersive regime and tends to the case of the Markovian limit ( $\lambda_v \rightarrow \infty$ ). We choose the parameter  $\omega_c = 0.1\omega_a$ ; the other parameters are the same as those in Fig. 2.

two non-Markovian environments (i.e.,  $\lambda_1 = \lambda_2 = 0.5\omega_a$ ) and shifts the frequency corresponding to the peak of the transmission in the dispersive regime compared with the Markovian approximation. We also consider another two asymmetric cases of  $\lambda_1 = 0.5\omega_a$  and  $\lambda_2 = 10\omega_a$  denoted by the green crosses and  $\lambda_1 = 10\omega_a$  and  $\lambda_2 = 300\omega_a$  denoted by the red circles, which show information similar to that of the cases of  $\lambda_1 = 0.5\omega_a$  and  $\lambda_2 = 300\omega_a$  denoted by the black dash-dotted line and  $\lambda_1 = \lambda_2 = 300\omega_a$  denoted by the black solid line, respectively.

Figure 7(a) shows that the sum of transmission and reflection  $|t_{cm}|^2 + |r_{cm}|^2$  is bounded by 1 in the Markovian regime because the SMB quantum system absorbs energy from the cavity when the cavity response is sensitive to the SMB quantum system and the information decays into the environments (for more details, see Appendix F). There also exist, however, regions in which

$$|t_c|^2 + |r_c|^2 > 1 \quad (33)$$

in the non-Markovian regime in Fig. 7(b) (for the derivations, see Appendix F). This special effect can be explained by the fact that the lost energy and information flow back to the hybrid system (SMB quantum system plus the cavity) from the non-Markovian environments, which indicates that the non-Markovianity can compensate the energy and information compared with the Markovian case.

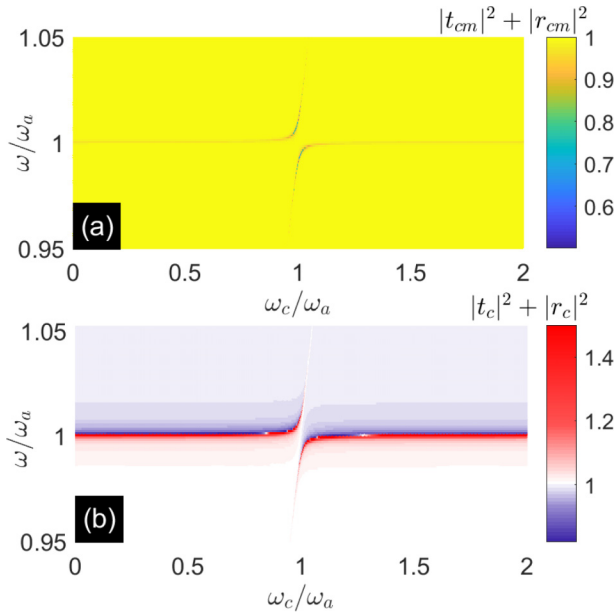


FIG. 7. Sum of the cavity transmission and reflection as a function of  $\omega$  and  $\omega_c$  in (a) the Markovian regime given by Eq. (24) ( $\lambda_1 = \lambda_2 = 300\omega_a$ ) and (b) the non-Markovian regime given by Eq. (23) ( $\lambda_1 = \lambda_2 = 0.5\omega_a$ ), demonstrating the energy absorption (blue) and emission (red). All other parameters are the same as those in Fig. 2.

## VI. GENERALIZATION TO THE PERIODICALLY DRIVEN SMB QUANTUM SYSTEM

In this section we consider that the non-Markovian dispersive readout may generalize to the periodically driven SMB quantum system [20,21,120], in which the cavity response is different from that in the time-independent system. For a periodically time-dependent system with driving frequency  $\Omega = 2\pi/T$ , the evaluation of Eq. (19) is hindered by the fact that the susceptibility  $\chi(t, t')$  generally depends on both times. However, time periodicity allows a simplification in the long-time limit, because after a transient stage, the  $T$  periodicity of the Hamiltonian  $\hat{H}_0(t)$  leads to  $\chi(t, t') = \chi(t + T, t' + T)$  [120]. Therefore, introducing the time difference  $\tau = t - t'$  allows one to conclude that  $\chi(t, t - \tau)$  is  $T$  periodic in time  $t$  such that it can be written as a combination of the Fourier series and integral, i.e.,

$$\chi(t, t - \tau) = \sum_k \int \frac{d\omega}{2\pi} e^{-ik\Omega t - i\omega\tau} \chi^{(k)}(\omega), \quad (34)$$

where  $k$  is an integer, i.e.,  $k = 0, \pm 1, \pm 2, \pm 3, \dots$ . Equation (34) implies the Fourier representation of Eq. (18) as  $O(\omega) = g \sum_k \chi^{(k)}(\omega - k\Omega)[a(\omega - k\Omega) + a^*(-\omega + k\Omega)]$ , which reflects the frequency mixing inherent in the linear response of the driven SMB quantum system. In the good cavity limit  $\Gamma \ll \omega_a, \Omega$ , together with Eq. (22), we can safely neglect the terms  $a^*(-\omega + k\Omega)$ . Therefore, we have

$$O(\omega) = g \sum_k \chi^{(k)}(\omega - k\Omega)a(\omega - k\Omega). \quad (35)$$

The computation of  $\chi^{(k)}(\omega)$  [121] starts by solving  $[\hat{H}_0(t) - i\partial_t]|u_m(t)\rangle = s_m|u_m(t)\rangle$  in the extended Hilbert space [122–127] to obtain the Floquet states  $|u_m(t)\rangle = |u_m(t + T)\rangle$  and the stationary solutions of the Schrödinger equation  $|\psi_m(t)\rangle = e^{-is_m t}|u_m(t)\rangle$  with the quasienergy  $s_m$ . The corresponding expression for the propagator  $U(t, t') = \sum_m e^{-is_m(t-t')}|u_m(t)\rangle\langle u_m(t')|$  allows us to deal with the operators in  $\chi(t, t')$ . Moreover, the periodically driven SMB quantum system [121] in the basis formed by the Floquet states can be written as  $\rho_0(t) = \sum_m p_m|u_m(t)\rangle\langle u_m(t)|$ , with  $p_m$  the occupation probability of the Floquet states [21]. With these components, we find from Eq. (34) the susceptibility

$$\chi^{(k)}(\omega) = \sum_{m,n,k'} \frac{(p_m - p_n)O_{mn,k'}^* O_{mn,k'}}{\omega + s_m - s_n + k'\Omega + i\gamma_{mn}/2}, \quad (36)$$

where  $O_{mn,k}$  denotes the  $k$ th Fourier component of the  $T$ -periodic transition matrix element  $O_{mn}(t) = \langle u_m(t)|\hat{O}|u_n(t)\rangle$ , i.e.,  $O_{mn,k} = \int_0^T \frac{dt}{T} e^{ik\Omega t} \langle u_m(t)|\hat{O}|u_n(t)\rangle$ , in which the level broadening  $\gamma_{mn}$  of the Floquet states has been introduced phenomenologically.

When the cavity frequency matches the level energy difference, Eq. (27) predicts a signal for the time-independent system. Moreover, we can also obtain the natural generalization to the periodically driven SMB quantum system, namely, that the level energy is replaced by the quasienergy shifted by multiples of the driving frequency  $\Omega$ . In this case, by iterating Eq. (20) with Eq. (35), we obtain

$$a(\omega) = \frac{i\tilde{\kappa}_1(\omega)[a_{\text{in}}^{(1)}(\omega) - a_{\text{in}}^{(1)}(i\lambda_1)]}{\omega_a - \omega + g^2\chi^{(0)}(\omega) - i[f_1(\omega) + f_2(\omega)]} - \frac{ig^2}{\omega_a - \omega + g^2\chi^{(0)}(\omega) - i[f_1(\omega) + f_2(\omega)]} \sum_{k \neq 0} \frac{\chi^{(k)}(\omega - k\Omega)\tilde{\kappa}_1(\omega - k\Omega)[a_{\text{in}}^{(1)}(\omega - k\Omega) - a_{\text{in}}^{(1)}(i\lambda_1)]}{\omega_a - \omega + k\Omega + g^2\chi^{(0)}(\omega - k\Omega) - i[f_1(\omega - k\Omega) + f_2(\omega - k\Omega)]} + \frac{g^4}{\omega_a - \omega + g^2\chi^{(0)}(\omega) - i[f_1(\omega) + f_2(\omega)]} \sum_{k \neq 0} \frac{\chi^{(k)}(\omega - k\Omega) \sum_{k_1 \neq 0} \chi^{(k_1)}(\omega - 2k_1\Omega)a(\omega - 2k_1\Omega)}{\omega_a - \omega + k\Omega + g^2\chi^{(0)}(\omega - k\Omega) - i[f_1(\omega - k\Omega) + f_2(\omega - k\Omega)]}. \quad (37)$$

With Eq. (12), the non-Markovian transmission for the Floquet periodically driven SMB quantum system can be written as

$$|t_c| \sim \frac{i\tilde{\kappa}_1(\omega)\kappa_2(-\omega)}{\omega_a - \omega + g^2\chi^{(0)}(\omega) - i[f_1(\omega) + f_2(\omega)]} - \frac{ig^2\kappa_2(-\omega)}{\omega_a - \omega + g^2\chi^{(0)}(\omega) - i[f_1(\omega) + f_2(\omega)]} \\ \times \sum_{k \neq 0} \frac{\chi^{(k)}(\omega - k\Omega)\tilde{\kappa}_1(\omega - k\Omega)}{\omega_a - \omega + k\Omega + g^2\chi^{(0)}(\omega - k\Omega) - i[f_1(\omega - k\Omega) + f_2(\omega - k\Omega)]} + \mathcal{O}(g^4), \quad (38)$$

where we have used approximation  $a_{\text{in}}^{(1)}(\omega - k\Omega) \sim a_{\text{in}}^{(1)}(\omega)$ . In Fig. 8(a) we plot the non-Markovian transmission  $|t_c|^2$  given by Eq. (38) as a function of  $\omega$  at zero temperature in the Floquet periodically driven SMB quantum system, where the SMB quantum system Hamiltonian becomes  $\hat{H}_0(t) = \omega_d(t)\hat{c}^\dagger\hat{c}$ . In this case, we take the periodic modulation as

$$\omega_d(t) = \omega_c + B \sin(\Omega t), \quad (39)$$

where  $B$  and  $\Omega$  are the amplitude and frequency (the corresponding period is  $T = 2\pi/\Omega$ ) of the periodic modulation, respectively. We can calculate the corresponding Floquet states for the periodic modulation given by Eq. (39) as  $|u_m(t)\rangle = e^{imB[\cos(\Omega t) - 1]/\Omega}|m\rangle$  with  $s_m = \omega_c m$ , where  $|m\rangle$  is

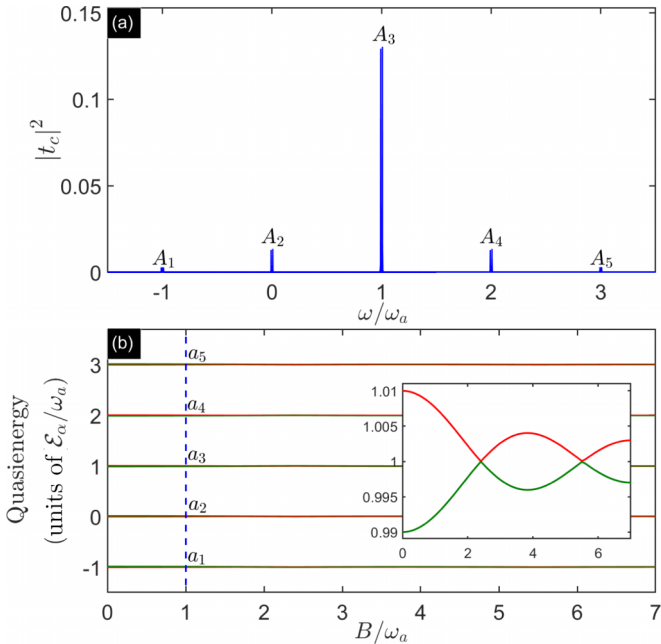


FIG. 8. (a) Non-Markovian transmission  $|t_c|^2$  given by Eq. (38) as a function of  $\omega$  at zero temperature in the Floquet periodically driven SMB quantum system, where the SMB quantum system Hamiltonian becomes  $\hat{H}_0(t) = \omega_d(t)\hat{c}^\dagger\hat{c}$ . In this case, we take the periodic modulation as  $\omega_d(t) = \omega_c + B \sin(\Omega t)$ , where  $B$  and  $\Omega$  are the amplitude and frequency (the corresponding period is  $T = 2\pi/\Omega$ ), respectively. Here we set  $B = \omega_a$  and  $\Omega = \omega_a$ . (b) Quasienergy  $\mathcal{E}_\alpha$  of the Floquet periodically driven RWA Hamiltonian  $\hat{H}_S(t) = \omega_a\hat{a}^\dagger\hat{a} + g(\hat{c}\hat{a}^\dagger + \hat{c}^\dagger\hat{a}) + \omega_d(t)\hat{c}^\dagger\hat{c}$  [ $\omega_c \rightarrow \omega_d(t)$  and  $\hat{H}_S \rightarrow \hat{H}_S(t)$  in Eq. (1)] with different modulation amplitudes  $B$ . The inset is an enlargement at the region  $\mathcal{E}_\alpha \sim \omega_a$  in (b). The other parameters are  $\omega_c = \omega_a$ ,  $\Gamma_1 = \Gamma_2 = \Gamma/2$ ,  $g = 0.01\omega_a$ ,  $\lambda = 1.3\omega_a$ , and  $\gamma_{mn} = 0.001\omega_c$ .

the eigenstate of  $\hat{H}_0(0)$ . Here we set  $B = \omega_a$  and  $\Omega = \omega_a$ . We show that the non-Markovian transmission  $|t_c|^2$  exhibits a series of peaks with period  $\Omega$  as the driving frequency  $\omega$  changes, where the horizontal ordinates (corresponding to the driving frequency  $\omega$ ) of the peaks  $A_1$ – $A_5$  correspond to the vertical ordinates (corresponding to the quasienergy  $\mathcal{E}_\alpha$ ) of points  $a_1$ – $a_5$  in Fig. 8(b). From Eq. (38) we show that the primary resonance peak corresponds to the first term of Eq. (38) near  $\omega \sim \omega_a$ , while the secondary resonance peak occurs in the second term of Eq. (38) for  $k = \pm 1$  at  $\omega \sim \omega_a \pm \Omega$ . Accordingly, the third resonance peak can be found at  $\omega \sim \omega_a \pm 2\Omega$ , which corresponds to the second term of Eq. (38), but with  $k = \pm 2$ . Interestingly, from Fig. 8(a) we find that the values of the second ( $\omega \sim \omega_a \pm \Omega$ ) and third ( $\omega \sim \omega_a \pm 2\Omega$ ) resonance peaks are much smaller than those of the primary resonance peak ( $\omega \sim \omega_a$ ), which originate from the nonresonance term  $\frac{ig^2\kappa_2(\omega)}{\omega_a - \omega + g^2\chi^{(0)}(\omega) - i[f_1(\omega) + f_2(\omega)]}$  being much smaller than  $\frac{i\tilde{\kappa}_1(\omega)\kappa_2(\omega)}{\omega_a - \omega + g^2\chi^{(0)}(\omega) - i[f_1(\omega) + f_2(\omega)]}$  at  $\omega \sim \omega_a \pm \Omega$  and  $\omega \sim \omega_a \pm 2\Omega$  in Eq. (38).

The influences of the different modulation amplitudes  $B$  on the non-Markovian transmission can be found in Figs. 9(a)–9(d), which for clarity are confined near the primary resonance peak ( $\omega \sim \omega_a$ ). As expected, we show that the non-Markovian transmission decreases in value compared with the Markovian limit [see the red solid and blue dotted lines in Figs. 9(a)–9(d)]. It is interesting that we find the width  $L_1 = 0.02\omega_a$  (difference of horizontal ordinates between two points  $x_1$  and  $x_2$ ) between two peaks marked by  $x_1$  and  $x_2$  equals  $\bar{L}_1 = 0.02\omega_a$  (difference of vertical ordinates between two points  $\bar{x}_1$  and  $\bar{x}_2$ ) between  $\bar{x}_1$  and  $\bar{x}_2$  for the Floquet quasienergy in Fig. 9(e) at  $B = 0$ . For the different modulation amplitudes  $B$  ( $B = \omega_a, 2\omega_a$ , and  $4\omega_a$ ), we have similar observations [see  $L_2 = \bar{L}_2 = 0.0157\omega_a$ ,  $L_3 = \bar{L}_3 = 0.0043\omega_a$ , and  $L_4 = \bar{L}_4 = 0.008\omega_a$  in Figs. 9(b)–9(e)]. This means that the Floquet quasienergy can be read out from the non-Markovian transmission.

## VII. NON-MARKOVIAN DISPERSIVE READOUT FOR THE QUANTUM NETWORK

In this section we generalize the results of non-Markovian dispersive readout to a more general network [128–132] involving two systems and cavities. A quantum network composed of the sending and receiving nodes, a quantum channel (optical fibers or waveguides), and an optical circulator are shown in Fig. 10. The sending and receiving node is made up of a quantum system in a cavity. The generated photons from the first quantum system leak out of the first cavity, propagate as a wave packet along the transmission line, and

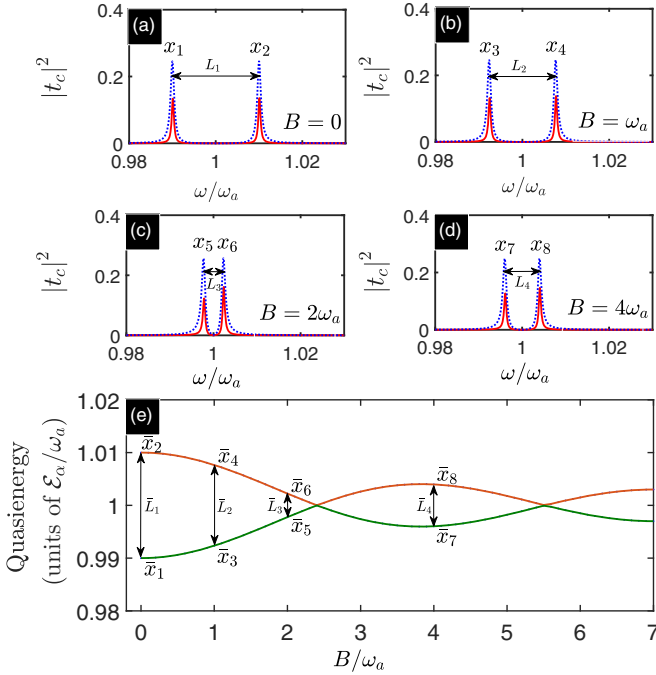


FIG. 9. (a)–(d) Non-Markovian transmission  $|t_c|^2$  given by Eq. (38) as a function of  $\omega$  at zero temperature in the Floquet periodically driven SMB quantum system with different modulation amplitudes  $B$ . The red solid and blue dotted lines correspond to  $\lambda = 1.3\omega_a$  and  $\lambda = 300\omega_a$ , respectively. (e) Quasienergy  $\mathcal{E}_\alpha$  of the Floquet periodically driven RWA Hamiltonian  $\hat{H}_S(t) = \omega_a \hat{a}^\dagger \hat{a} + g(\hat{c} \hat{a}^\dagger + \hat{c}^\dagger \hat{a}) + \omega_d(t) \hat{c}^\dagger \hat{c}$  with different modulation amplitudes  $B$ . We find  $L_1 = \bar{L}_1 = 0.02\omega_a$ ,  $L_2 = \bar{L}_2 = 0.0157\omega_a$ ,  $L_3 = \bar{L}_3 = 0.0043\omega_a$ , and  $L_4 = \bar{L}_4 = 0.008\omega_a$ . The other parameters are  $\Omega = \omega_a$ ,  $\omega_c = \omega_a$ ,  $\Gamma_1 = \Gamma_2 = \Gamma/2$ ,  $g = 0.01\omega_a$ , and  $\gamma_{mn} = 0.001\omega_c$ .

enter the second cavity. Finally, the optical state of the second cavity is transferred to the second quantum system. The total Hamiltonian (see Fig. 10) is given by

$$\hat{H}' = \hat{H}'_S + \hat{H}'_I, \quad (40)$$

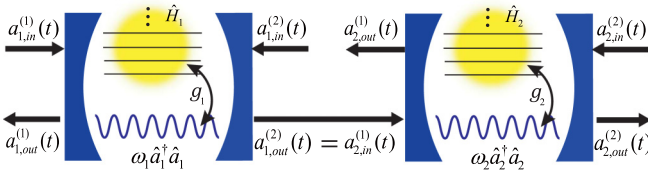


FIG. 10. Non-Markovian dispersive readout for a quantum network consisting of two cavities with frequency  $\omega_m$  ( $m = 1, 2$ ) coupled with quantum systems with frequency  $\Omega_m$  and interacting with two non-Markovian environments (modeled as harmonic oscillators with frequencies  $\omega_{m,k}$  and  $W_{m,k}$ ) with coupling coefficients  $V_{m,k}$  and  $G_{m,k}$ . The two cavities are connected by a quantized transmission line (or optical fiber). The susceptibility of the measured quantum network system can be obtained by the second cavity transmission  $t_{qn,c} = a_{2,out}^{(2)}(\omega)/a_{1,in}^{(1)}(\omega)$  and first cavity reflection  $r_{qn,c} = a_{1,out}^{(1)}(\omega)/a_{1,in}^{(1)}(\omega)$  amplitudes at frequency  $\omega$ . Here  $a_{m,in}^{(1)}(t)$  is in the vacuum state and does not contribute to the average output fields.

with

$$\begin{aligned} \hat{H}'_S &= \sum_m \omega_m \hat{a}_m^\dagger \hat{a}_m + \Omega_m \hat{c}_m^\dagger \hat{c}_m + g_m (\hat{c}_m + \hat{c}_m^\dagger) (\hat{a}_m + \hat{a}_m^\dagger), \\ \hat{H}'_I &= \sum_{m,k} \omega_{m,k} \hat{b}_{m,k}^\dagger \hat{b}_{m,k} + \sum_{m,k} (V_{m,k} \hat{a}_m \hat{b}_{m,k}^\dagger + V_{m,k}^* \hat{a}_m^\dagger \hat{b}_{m,k}) \\ &+ \sum_{m,k} W_{m,k} \hat{d}_{m,k}^\dagger \hat{d}_{m,k} + \sum_{m,k} (G_{m,k} \hat{a}_m \hat{d}_{m,k}^\dagger \\ &+ G_{m,k}^* \hat{a}_m^\dagger \hat{d}_{m,k}), \end{aligned} \quad (41)$$

where the first term of  $\hat{H}'_S$  in Eq. (41) is the free Hamiltonian of the  $m$ th cavity with frequency  $\omega_m$  ( $m = 1, 2$ ) and the second term of  $\hat{H}'_S$  in Eq. (41) denotes the free Hamiltonian of the  $m$ th quantum system with frequency  $\Omega_m$ . Here  $g_m$  is the coupling constant between the  $m$ th quantum system and the  $m$ th cavity. The  $m$ th cavity couples to the  $m$ th non-Markovian environments with eigenfrequencies  $\omega_{m,k}$  and  $W_{m,k}$ , which are modeled as collections of infinite modes via the creation (annihilation) operators  $\hat{b}_{m,k}^\dagger$  ( $\hat{b}_{m,k}$ ) and  $\hat{d}_{m,k}^\dagger$  ( $\hat{d}_{m,k}$ ). The parameters  $V_{m,k}$  and  $G_{m,k}$  are coupling coefficients between the two environments and the  $m$ th cavity, respectively. In this case, the non-Markovian Heisenberg-Langevin equation (7) is extended to

$$\begin{aligned} \frac{d}{dt} \hat{a}_m(t) &= -i\omega_m \hat{a}_m(t) - ig_m [\hat{c}_m(t) + \hat{c}_m^\dagger(t)] \\ &- \hat{K}_{m,1}^\dagger(t) - \hat{K}_{m,2}^\dagger(t) - \int_0^t d\tau \hat{a}_m(\tau) f_{m,1}(t - \tau) \\ &- \int_0^t d\tau \hat{a}_m(\tau) f_{m,2}(t - \tau), \end{aligned} \quad (42)$$

where the  $m$ th externally driven environment operators  $\hat{K}_{m,1}^\dagger(t) = i \sum_k V_{m,k}^* \hat{b}_{m,k}(0) e^{-i\omega_{m,k} t} = \int_{-\infty}^{\infty} d\tau \kappa_{m,1}^*(t - \tau) a_{m,in}^{(1)}(\tau)$  and  $\hat{K}_{m,2}^\dagger(t) = i \sum_k G_{m,k}^* \hat{d}_{m,k}(0) e^{-iW_{m,k} t} = \int_{-\infty}^{\infty} d\tau \kappa_{m,2}^*(t - \tau) a_{m,in}^{(2)}(\tau)$ . The  $m$ th cavity couples to the incoming and outgoing modes of environments at both ends; thus we define here the input-field operators as  $a_{m,in}^{(1)}(t) = \frac{1}{\sqrt{2\pi}} \sum_k e^{-i\omega_{m,k} t} \hat{b}_{m,k}(0)$  and  $a_{m,in}^{(2)}(t) = \frac{-1}{\sqrt{2\pi}} \sum_k e^{-iW_{m,k} t} \hat{d}_{m,k}(0)$  and the impulse response functions are  $\kappa_{m,1}(t) = \frac{-i}{\sqrt{2\pi}} \sum_k e^{i\omega_{m,k} t} V_{m,k}$  and  $\kappa_{m,2}(t) = \frac{i}{\sqrt{2\pi}} \sum_k e^{iW_{m,k} t} G_{m,k}$ . The correlation functions are given by

$$\begin{aligned} f_{m,1}(t) &= \sum_k |V_{m,k}|^2 e^{-i\omega_{m,k} t} = \int J_{m,1}(\omega) e^{-i\omega t} d\omega, \\ f_{m,2}(t) &= \sum_k |G_{m,k}|^2 e^{-iW_{m,k} t} = \int J_{m,2}(\omega) e^{-i\omega t} d\omega, \end{aligned} \quad (43)$$

where  $J_{m,1}(\omega) = \sum_k |V_{m,k}|^2 \delta(\omega - \omega_{m,k})$  and  $J_{m,2}(\omega) = \sum_k |G_{m,k}|^2 \delta(\omega - W_{m,k})$  represent the spectral densities of the two environments, respectively, and  $f_{m,1}(t)$  and  $f_{m,2}(t)$  denote the memory functions of the  $m$ th system, which describe the non-Markovian fluctuation-dissipation relationship of the environments.

Similar to Sec. III, we can obtain the non-Markovian input-output relations for the  $m$ th cavity mirror

$\nu$  ( $\nu = 1, 2$ ) (setting  $t_1 \rightarrow t$ ),

$$a_{m,\text{out}}^{(\nu)}(t) - a_{m,\text{in}}^{(\nu)}(t) = \int_0^t d\tau \kappa_{m,\nu}(\tau - t) \hat{a}_m(\tau), \quad (44)$$

where the output field of the first cavity constitutes the input field of the second cavity connected by a quantized transmission line, i.e.,

$$a_{1,\text{out}}^{(2)}(t) = a_{2,\text{in}}^{(1)}(t), \quad (45)$$

where  $a_{m,\text{out}}^{(1)}(t) = \frac{1}{\sqrt{2\pi}} \sum_k e^{-i\omega_k(t-t_1)} \hat{b}_{m,k}(t_1)$  and  $a_{m,\text{out}}^{(2)}(t) = \frac{-1}{\sqrt{2\pi}} \sum_k e^{-iW_{m,k}(t-t_1)} \hat{d}_{m,k}(t_1)$ .

$$t_{qn,c} = - \frac{\tilde{\kappa}_{1,1}(\omega)\kappa_{1,2}(-\omega)\tilde{\kappa}_{2,1}(\omega)\kappa_{2,2}(-\omega)}{\{\omega_1 - \omega - i[f_{1,1}(\omega) + f_{1,2}(\omega)] + g_1^2\chi_1(\omega)\}\{\omega_2 - \omega - i[f_{2,1}(\omega) + f_{2,2}(\omega)] + g_2^2\chi_2(\omega)\}}, \quad (46)$$

$$r_{qn,c} = \frac{i\tilde{\kappa}_{1,1}(\omega)\kappa_{1,1}(-\omega)}{\omega_1 - \omega - i[f_{1,1}(\omega) + f_{1,2}(\omega)] + g_1^2\chi_1(\omega)} + 1,$$

where  $\tilde{\kappa}_{m,\nu}(\omega) = \int_{-\infty}^0 \kappa_{m,\nu}^*(t') e^{i\omega t'} dt'$ ,  $a_{m,\text{in}}^{(\nu)}(\omega) = \int_0^{\infty} a_{m,\text{in}}^{(\nu)}(t') e^{i\omega t'} dt'$ ,  $f_{m,\nu}(\omega) = \int_0^{+\infty} f_{m,\nu}(t') e^{i\omega t'} dt'$ ,  $\kappa_{m,\nu}(\omega) = \int_{-\infty}^0 \kappa_{m,\nu}(t') e^{i\omega t'} dt'$ , and  $\chi_\alpha(\omega) = \sum_{m,n} \frac{(\rho_{\alpha,m} - \rho_{\alpha,n}) |O_{\alpha,mn}|^2}{\omega + E_{\alpha,m} - E_{\alpha,n} + i\gamma_{\alpha,mn}/2}$ , with the  $\alpha$ th SMB quantum system initially prepared in a thermal equilibrium state  $\rho_{\alpha,0} = \sum_n \rho_{\alpha,n} |n\rangle\langle n|$ ,  $\hat{H}_{\alpha,0} |n\rangle = E_{\alpha,n} |n\rangle$ , and the matrix element of the coupling operator satisfying  $O_{\alpha,mn} = \langle m | \hat{O}_\alpha | n \rangle = \langle m | \hat{c}_\alpha + \hat{c}_\alpha^\dagger | n \rangle$ , where  $\alpha = 1, 2$ . Here  $\gamma_{\alpha,mn}$  denotes the decay rate introduced phenomenologically. We show that the exact non-Markovian Heisenberg-Langevin equation (42) is the general one for the total system containing an arbitrary number of entangled modes coupled to an arbitrary number of photonic environments with arbitrary spectral densities at arbitrary initial temperatures beyond the RWA, which is not limited to the cases of the anisotropic non-rotating-wave approximation, i.e., all coupling including the cavity and environment in Eq. (41) might be of the form

$$\sum_n \nu_n (\hat{A}_n \hat{B}_n^\dagger + \hat{A}_n^\dagger \hat{B}_n) + \mu_n (\hat{A}_n \hat{B}_n + \hat{A}_n^\dagger \hat{B}_n^\dagger), \quad (47)$$

where  $\hat{A}_n^\dagger$  ( $\hat{A}_n$ ) and  $\hat{B}_n^\dagger$  ( $\hat{B}_n$ ) are the creation (annihilation) operators of the bosonic systems. Here  $\nu_n$  and  $\mu_n$  denote the coupling strengths of the rotating-wave and non-rotating-wave interactions, respectively. They allow one to investigate various exact non-Markovian dynamics in photonic systems. Applications of the readout for the non-Markovian quantum network cover various topics such as quantum information [133], quantum computation [134,135], quantum-to-classical transition [136,137], and quantum measurement [133,138].

### VIII. EXPERIMENTAL IMPLEMENTATION

In this section we discuss the feasibility of the experimental implementation in the optical cavity. For the model under study, we mainly focus on the following three points: (i) the interaction between the cavity and the SMB quantum system,

By solving the set of coupled-cavity differential equations (42) with the non-Markovian input-output relations (44), we can obtain the complete information for the quantum network of the coupled system cavities. Moreover, we can dispersively read out information of the two measured quantum systems from the transmission of the cavities [ $a_{1,\text{in}}^{(2)}(t)$  is assumed in the vacuum state] as follows: the transmission of the cavity  $\tilde{t}_{qn,c} = a_{2,\text{out}}^{(2)}(\omega)/a_{1,\text{in}}^{(1)}(\omega) = t_{qn,c} + \varphi_{qn,1}$  with  $\varphi_{qn,1} = -\phi_{qn}(\lambda_1, \omega) t_{qn,c}$  and  $\phi_{qn}(\lambda_1, \omega) = a_{1,\text{in}}^{(1)}(i\lambda_1)/a_{1,\text{in}}^{(1)}(\omega)$ , and reflection of cavity  $\tilde{r}_{qn,c} = a_{1,\text{out}}^{(1)}(\omega)/a_{1,\text{in}}^{(1)}(\omega) = r_{qn,c} + \varphi_{qn,2}$  with  $\varphi_{qn,2} = -\phi_{qn}(\lambda_1, \omega) r_{qn,c}$ , where

(ii) probing the effect of non-Markovian dynamics on the system's behavior, and (iii) the Lorentzian spectral density.

(i) From Eq. (2) we can see that the coupling between the cavity and the SMB quantum system is written in its full form without performing the RWA, which can be implemented by means of superconducting quantum interference devices (SQUIDs) [139–141]. The SQUID driven by external fluxes allows a modulation of the electrical boundary condition of the cavity and the interaction between the cavity and the SMB quantum system, provided the modulation frequency is smaller than the SQUID plasma frequency [139–141]. In addition, the coupling beyond the RWA can be realized by driving transversely the momentum states of atoms inside a cavity in the dispersive regime, which realizes the Dicke model [142].

(ii) The non-Markovian system under study describes the optical cavity coupled to the non-Markovian environments containing all feedback of the non-Markovian environments on the SMB quantum system, which can be implemented by the photonic structured reservoirs [143–155]. The spectral density of a condensed-matter heat bath can be obtained by observing the non-Markovian behavior of an optomechanical resonator coupled to it, which has been measured through the emitted light of a micro-optomechanical system by the system identification approach in experiment [81]. The demonstration equipment consists of a thick layer of  $\text{Si}_3\text{N}_4$  with a high-reflectivity mirror pad at its center, as a mechanically moving end mirror in a Fabry-Pérot cavity [81]. Other references about the non-Markovian experiments can be found in Refs. [156–161]. Thus we can detect what kind of spectral density the environments belong to by the above experimental methods.

(iii) For the Lorentzian spectral density, we make use of the so-called pseudomode theory developed in Refs. [162–169] to clarify how the decayed information can flow back to the system. According to the pseudomode theory [162–169], pseudomodes of an environment are auxiliary variables, which are introduced in terms of the position of the poles of the environment's spectral function. The interaction between the cavity and environments can be considered to be

a coherent interaction between the cavity mode and pseudomodes, which are surrounded by the external Markovian environments known as the pseudomodes' environments. By adding pseudomodes to the cavity as a hybrid quantum system, an exact non-Markovian input-output relation with Lorentzian spectral density can be obtained. Also, for the quantum noise of the system in the case of the vacuum state of the environment, the cavity mode undergoes a Gaussian Ornstein-Uhlenbeck process, which corresponds to the Lorentzian spectral density [107–109].

Finally, we suggest that the non-Markovian dispersive readout may be realized by considering an optical cavity implemented by a SQUID and coupling with the Lorentz-type spectral density environments (which are realized by the pseudomode method or Gaussian Ornstein-Uhlenbeck process), where the optical cavity is driven by the external electric field. In this sense, it is possible to achieve the theoretical scheme within the current experimental technology.

## IX. CONCLUSION

In this paper we have developed the theory for dispersive readout in the non-Markovian regime by taking the non-Markovianity into account. Based on the nonequilibrium linear response theory, the susceptibility of the SMB quantum system to be measured is obtained by setting thermal equilibrium state as the initial state of the SMB quantum system. Furthermore, the cavity transmission given by the SMB quantum system susceptibility shifts the frequency corresponding to the peak in the dispersive regime and the input-output relations in both Markovian and non-Markovian cases have been derived. The treatment approach enables straightforward calculations, in particular the treatment beyond a rotating-wave approximation. Moreover, we made possible generalization of the non-Markovian dispersive readout theory to the periodically driven SMB quantum system based on the Floquet treatment approach [20,21,122–127] and quantum network [128–132]. The corresponding experimental implementation of the model system is possible and feasible.

The formalism presented in this paper opens an alternative field of possible applications for the quantum information [29,170–172] and quantum communication [173], which makes it possible to better understand the relation between the dispersive measurement [174–176] and non-Markovianity [177–180]. Our results might also be extended to a wide class of open quantum systems with (i) a second-order nonlinear medium  $\Omega(\hat{a}^2\hat{c}^\dagger + \hat{c}\hat{a}^{\dagger 2})$ , (ii) third-order nonlinear materials  $J\hat{b}^{\dagger 2}\hat{b}^2$ , (iii) Jaynes-Cummings models  $\sum_k V_k(\sigma_- a_k^\dagger + a_k \sigma_+)$  [181–186] or Rabi models  $\sum_k G_k \sigma_x (a_k^\dagger + a_k)$  [187,188], and (iv) optomechanical couplings with a linear term  $U\hat{a}^\dagger\hat{a}(\hat{b} + \hat{b}^\dagger)$  [189–191] or quadratic term  $U\hat{a}^\dagger\hat{a}(\hat{b} + \hat{b}^\dagger)^2$  [53,54,192–195] interacting with non-Markovian reservoirs, which deserve future studies. Possible applications include using the cavity as a quantum bus to couple widely separated qubits in a quantum computer or as a quantum memory [196] to store quantum information or even as a generator and detector of single microwave photons for quantum communication, which also open up many different possibilities for quantum optical experiments with circuits [14,44,57,197].

## ACKNOWLEDGMENTS

H.Z.S. would like to thank Dr. Jin-Feng Yang for valuable and constructive discussions. This work was supported by National Natural Science Foundation of China under Grants No. 12175033 and No. 12147206, and Natural Science Foundation of Jilin Province (subject arrangement project) under Grant No. 20210101406JC.

## APPENDIX A: DERIVATION OF EQ. (16)

In the classical limit  $a(t) \equiv \langle \hat{a}(t) \rangle$ , we are not interested in quantum fluctuations of the cavity field and rewrite Eq. (1) as

$$\hat{H}_S = \hat{H}_0 + \hat{H}_{\text{ex}}(t), \quad (\text{A1})$$

where  $\hat{H}_0 = \omega_c \hat{c}^\dagger \hat{c}$  describes system Hamiltonian in the absence of the cavity. Here  $\hat{H}_{\text{ex}}(t) = \hat{O}F(t)$ , with  $F(t) = g[a(t) + a^*(t)]$ , defines the SMB quantum system experiencing an additional driving from the cavity compared to the case without the cavity. We assume that  $\rho(t)$  is the total density matrix and its dynamics is determined by

$$\dot{\rho}(t) = -i[\hat{H}_S, \rho(t)] \equiv -i\hat{L}(t)\rho(t), \quad (\text{A2})$$

where the Hamiltonian  $\hat{H}_S$  is given by Eq. (A1) and  $\hat{L}(t)$  describes the total Liouville operator. When the cavity is absent, there is only the bosonic system  $\hat{H}_0$  left and the total density matrix becomes  $\rho_0(t)$ , which is determined by

$$\dot{\rho}_0(t) = -i[\hat{H}_0, \rho_0(t)] \equiv -i\hat{L}_0(t)\rho_0(t). \quad (\text{A3})$$

Considering an observable  $\hat{O}(t)$  of the SMB quantum system, we are interested in the change rate of  $\hat{O}(t)$  due to the presence of the cavity. To calculate the change rate, we divide the total density matrix into two parts with the existence of the cavity [113,198,199]

$$\rho(t) = \rho_0(t) + \rho_{\text{ex}}(t), \quad (\text{A4})$$

where  $\rho_0(t)$ , determined by Eq. (A3), denotes the density matrix corresponding to the absence of the cavity with the initial condition  $\rho(0) = \rho_0(0)$  and  $\rho_{\text{ex}}(t)$  corresponds to the change of  $\rho(t)$  due to the cavity, where  $\rho_{\text{ex}}(0) = 0$ . Similar to Eq. (A4), the Liouville operator can be divided into

$$\hat{L}(t) = \hat{L}_0(t) + \hat{L}_{\text{ex}}(t), \quad (\text{A5})$$

where  $\hat{L}_0(t)$  denotes the Liouville operator corresponding to the absence of the cavity and  $\hat{L}_{\text{ex}}(t)$  means the change of  $\hat{L}(t)$  due to the existence of the cavity determined by  $\hat{L}_{\text{ex}}(t)\rho_0(t) = [\hat{H}_{\text{ex}}(t), \rho_0(t)]$ . Substituting Eqs. (A4) and (A5) into Eq. (A2), we can obtain

$$\begin{aligned} \dot{\rho}(t) &= -i\hat{L}(t)\rho(t) \\ &= -i\hat{L}_0(t)\rho_0(t) - i\hat{L}_0(t)\rho_{\text{ex}}(t) \\ &\quad - i\hat{L}_{\text{ex}}(t)\rho_0(t) - i\hat{L}_{\text{ex}}(t)\rho_{\text{ex}}(t) \\ &\equiv \dot{\rho}_0(t) + \dot{\rho}_{\text{ex}}(t). \end{aligned} \quad (\text{A6})$$

With Eq. (A3) and neglecting the second-order term  $-i\hat{L}_{\text{ex}}(t)\rho_{\text{ex}}(t)$  of Eq. (A6), we can obtain Eq. (16).

### APPENDIX B : RWA OF THE NON-MARKOVIAN CAVITY MODE

When considering the treatment of the non-Markovian cavity transmission given by (23) beyond the RWA, neglecting in Eq. (21) the contribution with  $a^*(-\omega)$  represents a RWA for the cavity mode. With Eq. (21) for the cavity amplitude  $a(\omega)$  together with the corresponding equation for  $a^*(-\omega)$ , we obtain

$$N \begin{pmatrix} a(\omega) \\ a^*(-\omega) \end{pmatrix} = \begin{pmatrix} i\tilde{\kappa}_1(\omega)a_{\text{in}}^{(1)}(\omega) \\ i\tilde{\kappa}_1^*(-\omega)a_{\text{in}}^{(1)*}(-\omega) \end{pmatrix} \quad (\text{B1})$$

or

$$\begin{pmatrix} a(\omega) \\ a^*(-\omega) \end{pmatrix} = N^{-1} \begin{pmatrix} i\tilde{\kappa}_1(\omega)a_{\text{in}}^{(1)}(\omega) \\ i\tilde{\kappa}_1^*(-\omega)a_{\text{in}}^{(1)*}(-\omega) \end{pmatrix}, \quad (\text{B2})$$

with the matrix

$$N = \begin{pmatrix} C(\omega) & g^2\chi(\omega) \\ -g^2\chi^*(-\omega) & -C^*(-\omega) \end{pmatrix}, \quad (\text{B3})$$

where  $C(\omega) = \omega_a - \omega + g^2\chi(\omega) - i[f_1(\omega) + f_2(\omega)]$ , and the inverse matrix of  $N$  can be written as

$$N^{-1} = \begin{pmatrix} a_{11} & a_{12} \\ a_{21} & a_{22} \end{pmatrix}, \quad (\text{B4})$$

where  $a_{11} = -C^*(-\omega)/[g^4\chi(\omega)\chi^*(-\omega) - C(\omega)C^*(-\omega)]$ ,  $a_{12} = -g^2\chi(\omega)/[g^4\chi(\omega)\chi^*(-\omega) - C(\omega)C^*(-\omega)]$ ,  $a_{21} = g^2\chi^*(-\omega)/[g^4\chi(\omega)\chi^*(-\omega) - C(\omega)C^*(-\omega)]$ , and  $a_{22} = C(\omega)/[g^4\chi(\omega)\chi^*(-\omega) - C(\omega)C^*(-\omega)]$ . We impose that  $a_{12}$ ,  $a_{21}$ , and  $a_{22}$  tend to zero when  $|C(\omega)|$  and  $|g^2\chi(\omega)|$  are much smaller than  $|C^*(-\omega)|$ , which requires that (i) the cavity is driven close to resonance ( $|\omega - \omega_a| \ll \omega_a$ ), (ii) the high-finesse cavity ( $|\omega_a/[f_1(\omega) + f_2(\omega)]| \gg 1$ ) is satisfied, and (iii)  $|g^2\chi(\omega)|$  is much smaller than the bare cavity frequency  $\omega_a$ , which lead to Eq. (22). In this case, we have  $a_{11} \approx C(\omega)^{-1}$  due to  $g^4\chi(\omega)\chi^*(-\omega) \approx 0$ . Then the inverse matrix (B4) of  $N$  is approximately given by

$$N^{-1} \approx \begin{pmatrix} C(\omega)^{-1} & 0 \\ 0 & 0 \end{pmatrix}, \quad (\text{B5})$$

where the corrections are of higher order in the small frequencies on the left-hand side of Eq. (22). Computing  $a(\omega)$  with this expression for  $N^{-1}$  is equivalent to ignoring  $a^*(-\omega)$  in Eq. (21).

### APPENDIX C: SUSCEPTIBILITY UNDER THE RWA

For the RWA case, the Hamiltonian  $\hat{H}_S$  in Eq. (1) can be rewritten as

$$\hat{H}_S = \omega_a \hat{a}^\dagger \hat{a} + g(\hat{c} \hat{a}^\dagger + \hat{c}^\dagger \hat{a}) + \omega_c \hat{c}^\dagger \hat{c}, \quad (\text{C1})$$

which leads to Eq. (7) becoming

$$\begin{aligned} \frac{d}{dt} \hat{a}(t) &= -i\omega_a \hat{a}(t) - ig\hat{c}(t) - \hat{K}_1^\dagger(t) - \hat{K}_2^\dagger(t) \\ &\quad - \int_0^t d\tau \hat{a}(\tau) f_1(t - \tau) - \int_0^t d\tau \hat{a}(\tau) f_2(t - \tau). \end{aligned} \quad (\text{C2})$$

In the classical limit, Eq. (C1) can be written as  $\hat{H}_S = \hat{H}_0 + \hat{H}_{\text{ex}}(t)$ , with  $\hat{H}_0 = \omega_c \hat{c}^\dagger \hat{c}$ , and the corresponding perturbation Hamiltonian with the RWA is

$$\hat{H}_{\text{ex}}(t) = g[\hat{c}a^*(t) + \hat{c}^\dagger a(t)] \equiv g \sum_{j=1,2} \hat{c}_j F_j(t), \quad (\text{C3})$$

where  $\hat{c}_1 = \hat{c}$ ,  $F_1(t) = a^*(t)$ ,  $\hat{c}_2 = \hat{c}^\dagger$ , and  $F_2(t) = a(t)$ . With  $\rho_{\text{ex}}(t)$  given by Eq. (17), the change rate of the expectation value for the operator  $\hat{c}$  in Eq. (C2) due to the cavity is given by

$$c(t) \equiv \text{Tr}\{\hat{c}\rho_{\text{ex}}(t)\} = \sum_{j=1,2} \int_0^t dt' g F_j(t') \chi_{c_j}(t, t'), \quad (\text{C4})$$

with the susceptibility

$$\chi_{c_j}(t, t') = -i \text{Tr}\{[\hat{c}(t), \hat{c}_j(t')]\rho_0\} \theta(t - t'), \quad (\text{C5})$$

where  $\hat{c}(t) = e^{i\hat{H}_0 t} \hat{c} e^{-i\hat{H}_0 t}$ , with  $\hat{H}_0 = \omega_c \hat{c}^\dagger \hat{c}$ . We assume that the initial SMB quantum system density operator is prepared in a thermal equilibrium state (25). After some simple algebra, we can obtain

$$\begin{aligned} \chi_{c1}(t, t') &= -i \sum_{m,n} (p_m - p_n) e^{i(E_m - E_n)(t - t')} c_{mn} c_{nm} \theta(t - t'), \\ \chi_{c2}(t, t') &= -i \sum_{m,n} (p_m - p_n) e^{i(E_m - E_n)(t - t')} |c_{mn}|^2 \theta(t - t'). \end{aligned} \quad (\text{C6})$$

With  $c_{mn} c_{nm} = 0$  and  $|c_{mn}|^2 = |\sqrt{n} \delta_{m,n-1}|^2$  due to  $c_{mn} = \langle m | \hat{c} | n \rangle = \sqrt{n} \delta_{m,n-1}$  and  $c_{nm} = \langle n | \hat{c}^\dagger | m \rangle = \sqrt{m} \delta_{n,m-1}$ , we obtain  $\chi_{c1}(t) = 0$ . In this case, Eq. (C4) becomes

$$c(t) = \int_0^t dt' g a(t') \chi(t - t'), \quad (\text{C7})$$

where we have defined

$$\begin{aligned} \chi(t - t') &\equiv \chi_{c2}(t - t') \\ &= -i \sum_{m,n} (p_m - p_n) e^{i(E_m - E_n)(t - t')} |c_{mn}|^2 \theta(t - t'). \end{aligned} \quad (\text{C8})$$

With modified Laplace transformation, the susceptibility can be written as

$$\chi(\omega) = \sum_{m,n} \frac{(p_m - p_n) |c_{mn}|^2}{\omega + E_m - E_n + i\gamma_{mn}/2}, \quad (\text{C9})$$

where  $\gamma_{mn}$  denotes the decay rate introduced phenomenologically. Equation (C7) is a convolution and in frequency space reads  $c(\omega) = g\chi(\omega)a(\omega)$ . With  $|c_{mn}|^2 = n|\delta_{m,n-1}|^2$ , Eq. (C9) is simplified to

$$\chi(\omega) = \sum_n \frac{(p_{n-1} - p_n)n}{\omega + E_{n-1} - E_n + i\gamma_{n-1,n}/2}, \quad (\text{C10})$$

which can return to the RWA result, i.e., the first term of Eq. (27).

#### APPENDIX D: RELEVANT PROOFS FOR THE MARKOVIAN REGIME

##### 1. The imaginary part of the susceptibility is less than zero for the whole parameter regime

The susceptibility given by Eq. (26) can be rewritten as

$$\chi(\omega) = \sum_{m,n} \frac{c_{mn}a_{mn}}{a_{mn}^2 + b^2} - i \frac{c_{mn}b}{a_{mn}^2 + b^2}, \quad (\text{D1})$$

where  $a_{mn} = \omega + E_m - E_n$ ,  $b = \gamma_{mn}/2 \equiv \gamma/2$  ( $\gamma$  is a constant decay),  $c_{mn} = (p_m - p_n)|O_{mn}|^2 \equiv -c_{nm}$  due to  $|O_{mn}|^2 = |\langle m|\hat{c} + \hat{c}^\dagger|n\rangle|^2 \equiv |O_{nm}|^2$ ,  $p_n = \frac{(\hat{c}^\dagger \hat{c})^n}{(1 + (\hat{c}^\dagger \hat{c})^n)^{n+1}}$ , and  $\langle \hat{c}^\dagger \hat{c} \rangle = (e^{\hbar\omega_c/\kappa_B T} - 1)^{-1}$ . The imaginary part of the susceptibility in Eq. (D1) is

$$\text{Im}[\chi(\omega)] = \sum_{m,n>m} X_{mn} \equiv - \sum_{m,n>m} \frac{c_{mn}b}{a_{mn}^2 + b^2} + \frac{c_{nm}b}{a_{nm}^2 + b^2}, \quad (\text{D2})$$

where

$$X_{mn} = - \frac{c_{mn}b}{a_{mn}^2 + b^2} + \frac{c_{nm}b}{a_{nm}^2 + b^2} = \frac{4bc_{mn}(E_m - E_n)\omega}{[b^2 + (\omega + E_m - E_n)^2][b^2 + (\omega - E_m + E_n)^2]}. \quad (\text{D3})$$

Now we discuss two situations: (1) If  $E_m < E_n$  or, equivalently,  $p_m > p_n$ , we have  $c_{mn} > 0$ , which leads to  $X_{mn} < 0$  or

$$\text{Im}[\chi(\omega)] < 0, \quad (\text{D4})$$

and (2) if  $E_m > E_n$  or, equivalently,  $p_m < p_n$ , we have  $c_{mn} < 0$ , which also leads to  $X_{mn} < 0$  or Eq. (D4).

##### 2. The sum of transmission and reflection is less than one for the whole parameter regime

We show that the susceptibility (26) is defined as  $\chi(\omega) \equiv x + iy$ , based on which the sum of transmission and reflection given by Eq. (24) can be written as

$$|r_{\text{cm}}|^2 + |t_{\text{cm}}|^2 = 1 + \frac{8\Gamma_1 y g^2}{4(\omega_a - \omega + x g^2)^2 + (\Gamma - 2y g^2)^2}, \quad (\text{D5})$$

which leads to the inequality given by Eq. (28) due to  $y = \text{Im}[\chi(\omega)] < 0$  proved by Eq. (D4) for the whole parameter regime in the Markovian approximation.

#### APPENDIX E: CONDITIONS FOR THE RWA

In this Appendix we give the justification of the conditions of the rotating-wave approximation as follows. We now rewrite the Hamiltonian (2) as

$$\hat{H}_S'' = \hat{H}_0'' + \varepsilon \hat{H}_I'', \quad (\text{E1})$$

with

$$\hat{H}_0'' = \omega_a \hat{a}^\dagger \hat{a} + \omega_c \hat{c}^\dagger \hat{c}, \quad (\text{E2})$$

$$\hat{H}_I'' = g(\hat{c} + \hat{c}^\dagger)(\hat{a} + \hat{a}^\dagger), \quad (\text{E3})$$

where  $\varepsilon$  stands for the interaction strength. In the interaction picture, we have

$$\hat{H}_I''(t) = g\hat{c}\hat{c}^\dagger e^{-i(\omega_a - \omega_c)t} + g\hat{a}\hat{c}e^{-i(\omega_a + \omega_c)t} + \text{H.c.}, \quad (\text{E4})$$

where H.c. denotes the Hermitian conjugate. The first few terms in the interacting strength  $\varepsilon$  of the time-evolution operator for Dyson expansion [200] is given by

$$\begin{aligned} U''(t) &= \mathcal{T} \exp \left[ -i\varepsilon \int_0^t \hat{H}_I''(t_1) dt_1 \right] \\ &= 1 - i\varepsilon \int_0^t \hat{H}_I''(t_1) dt_1 - \varepsilon^2 \int_0^t dt_1 \\ &\quad \times \int_0^{t_1} \hat{H}_I''(t_1) \hat{H}_I''(t_2) dt_2 + \dots \end{aligned} \quad (\text{E5})$$

Substituting Eq. (E4) into Eq. (E5), we can obtain

$$\begin{aligned} -i \int_0^t \hat{H}_I''(t_1) dt_1 &= \frac{g}{\omega_a - \omega_c} [e^{-i(\omega_a - \omega_c)t} - 1] \hat{a} \hat{c}^\dagger \\ &\quad - \frac{g}{\omega_a - \omega_c} [e^{i(\omega_a - \omega_c)t} - 1] \hat{a}^\dagger \hat{c} \\ &\quad + \frac{g}{\omega_a + \omega_c} [e^{-i(\omega_a + \omega_c)t} - 1] \hat{a} \hat{c} \\ &\quad - \frac{g}{\omega_a + \omega_c} [e^{i(\omega_a + \omega_c)t} - 1] \hat{a}^\dagger \hat{c}^\dagger. \end{aligned} \quad (\text{E6})$$

We show that the rotating-wave approximation requires

$$\begin{aligned} \frac{g}{\omega_a + \omega_c} &\ll 1, \\ \frac{g}{|\omega_a - \omega_c|} &\gg \frac{g}{\omega_a + \omega_c}, \end{aligned} \quad (\text{E7})$$

which lead to the condition (30) for the RWA. In this case, the counterrotating terms can be neglected. When the system parameters do not satisfy Eq. (E7), we cannot neglect the non-rotating-wave terms in the Hamiltonian (E4) and therefore this RWA breaks down.

#### APPENDIX F: RELEVANT PROOFS FOR THE NON-MARKOVIAN REGIME

In this case, we show that the non-Markovian transmission and reflection given by Eq. (23) can be revised to

$$\begin{aligned} t_c &= \frac{A + iB}{\omega_a - \omega + X + iY}, \\ r_c &= 1 + \frac{C + iD}{\omega_a - \omega + X + iY}, \end{aligned} \quad (\text{F1})$$

with the coefficients  $X = f_{1y}(\omega) + f_{2y}(\omega) + g^2 \text{Re}[\chi(\omega)]$ ,  $Y = -f_{1x}(\omega) - f_{2x}(\omega) + g^2 \text{Im}[\chi(\omega)]$ ,  $A = -\frac{\omega \sqrt{\Gamma_1 \Gamma_2} \lambda_1 \lambda_2 (\lambda_1 + \lambda_2)}{(\lambda_1^2 + \omega^2)(\lambda_2^2 + \omega^2)}$ ,  $B = -\frac{\sqrt{\Gamma_1 \Gamma_2} \lambda_1 \lambda_2 (\lambda_1 \lambda_2 - \omega^2)}{(\lambda_1^2 + \omega^2)(\lambda_2^2 + \omega^2)}$ ,  $C = \frac{2\Gamma_1 \omega \lambda_1^3}{(\lambda_1^2 - \omega^2)^2 + (2\omega \lambda_1)^2}$ , and  $D = \frac{\Gamma_1 \lambda_1^2 (\lambda_1^2 - \omega^2)}{(\lambda_1^2 - \omega^2)^2 + (2\omega \lambda_1)^2}$ , where  $f_{1x}(\omega)$  and  $f_{1y}(\omega)$  are the real and imaginary parts of  $f_1(\omega)$ , respectively, while  $f_{2x}(\omega)$  and  $f_{2y}(\omega)$  denote the real and imaginary parts of  $f_2(\omega)$ , respectively. Simple algebra to the sum of transmission and reflection obeys

$$|r_c|^2 + |t_c|^2 = 1 + \frac{A^2 + B^2 + C(C + 2Z) + D(D + 2Y)}{Z^2 + Y^2}, \quad (\text{F2})$$

where  $Z = X - \omega + \omega_a$ .

If the coefficients satisfy

$$A^2 + B^2 + C(C + 2Z) + D(D + 2Y) > 0 \quad (\text{F3})$$

or

$$\omega_a > -\frac{A^2 + B^2 + C(C - 2\omega + 2X) + D(D + 2Y)}{2C}, \quad (\text{F4})$$

we can obtain the inequality given by Eq. (33); otherwise  $|r_c|^2 + |t_c|^2 \leq 1$ , where  $C > 0$  in Eq. (F1) has been used. Here we show that the regime being greater than one for the sum of transmission and reflection in Fig. 7(b) falls into that given by Eq. (F3) or (F4).

- 
- [1] M. A. Nielsen and I. L. Chuang, *Quantum Computation and Quantum Information* (Cambridge University Press, Cambridge, 2000).
- [2] C. H. Bennett and D. P. DiVincenzo, Quantum information and computation, *Nature (London)* **404**, 247 (2000).
- [3] A. Steane, Quantum computing, *Rep. Prog. Phys.* **61**, 117 (1998).
- [4] R. J. Schoelkopf and S. M. Girvin, Wiring up quantum systems, *Nature (London)* **451**, 664 (2008).
- [5] Z.-L. Xiang, S. Ashhab, J. Q. You, and F. Nori, Hybrid quantum circuits: Superconducting circuits interacting with other quantum systems, *Rev. Mod. Phys.* **85**, 623 (2013).
- [6] G. Kurizki, P. Bertet, Y. Kubo, K. Mølmer, D. Petrosyan, P. Rabl, and J. Schmiedmayer, Quantum technologies with hybrid systems, *Proc. Natl. Acad. Sci. USA* **112**, 3866 (2015).
- [7] J. Gambetta, A. Blais, D. I. Schuster, A. Wallraff, L. Frunzio, J. Majer, M. H. Devoret, S. M. Girvin, and R. J. Schoelkopf, Qubit-photon interactions in a cavity: Measurement-induced dephasing and number splitting, *Phys. Rev. A* **74**, 042318 (2006).
- [8] A. Blais, J. Gambetta, A. Wallraff, D. I. Schuster, S. M. Girvin, M. H. Devoret, and R. J. Schoelkopf, Quantum-information processing with circuit quantum electrodynamics, *Phys. Rev. A* **75**, 032329 (2007).
- [9] G. Johansson, L. Tornberg, V. S. Shumeiko, and G. Wendin, Readout methods and devices for Josephson-junction-based solid-state qubits, *J. Phys.: Condens. Matter* **18**, S901 (2006).
- [10] G. Johansson, L. Tornberg, and C. M. Wilson, Fast quantum limited readout of a superconducting qubit using a slow oscillator, *Phys. Rev. B* **74**, 100504(R) (2006).
- [11] D. I. Schuster, A. A. Houck, J. A. Schreier, A. Wallraff, J. M. Gambetta, A. Blais, L. Frunzio, J. Majer, B. Johnson, M. H. Devoret, S. M. Girvin, and R. J. Schoelkopf, Resolving photon number states in a superconducting circuit, *Nature (London)* **445**, 515 (2007).
- [12] R. Bianchetti, S. Filipp, M. Baur, J. M. Fink, M. Göppl, P. J. Leek, L. Steffen, A. Blais, and A. Wallraff, Dynamics of dispersive single-qubit readout in circuit quantum electrodynamics, *Phys. Rev. A* **80**, 043840 (2009).
- [13] T. Wirth, J. Lisenfeld, A. Lukashenko, and A. V. Ustinov, Microwave readout scheme for a Josephson phase qubit, *Appl. Phys. Lett.* **97**, 262508 (2010).
- [14] A. Wallraff, D. I. Schuster, A. Blais, L. Frunzio, R. S. Huang, J. Majer, S. Kumar, S. M. Girvin, and R. J. Schoelkopf, Strong coupling of a single photon to a superconducting qubit using circuit quantum electrodynamics, *Nature (London)* **431**, 162 (2004).
- [15] A. Blais, R. S. Huang, A. Wallraff, S. M. Girvin, and R. J. Schoelkopf, Cavity quantum electrodynamics for superconducting electrical circuits: An architecture for quantum computation, *Phys. Rev. A* **69**, 062320 (2004).
- [16] E. A. Sete, J. M. Gambetta, and A. N. Korotkov, Purcell effect with microwave drive: Suppression of qubit relaxation rate, *Phys. Rev. B* **89**, 104516 (2014).
- [17] G. P. Berman, A. A. Chumak, and V. I. Tsifrinovich, Dynamics of a phase qubit-resonator system: Requirements for fast nondemolition readout of a phase qubit, *J. Low Temp. Phys.* **170**, 172 (2013).
- [18] G.-Q. Zhang, Y.-P. Wang, and J. Q. You, Dispersive readout of a weakly coupled qubit via the parity-time-symmetric phase transition, *Phys. Rev. A* **99**, 052341 (2019).
- [19] D. I. Schuster, Circuit quantum electrodynamics, Ph.D. thesis, Yale University, 2007.
- [20] S. Kohler, Dispersive Readout of Adiabatic Phases, *Phys. Rev. Lett.* **119**, 196802 (2017).
- [21] S. Kohler, Dispersive readout: Universal theory beyond the rotating-wave approximation, *Phys. Rev. A* **98**, 023849 (2018).
- [22] J. A. Haigh, N. J. Lambert, A. C. Doherty, and A. J. Ferguson, Dispersive readout of ferromagnetic resonance for strongly coupled magnons and microwave photons, *Phys. Rev. B* **91**, 104410 (2015).
- [23] S. Park, C. Metzger, L. Tosi, M. F. Goffman, C. Urbina, H. Pothier, and A. L. Yeyati, From Adiabatic to Dispersive Readout of Quantum Circuits, *Phys. Rev. Lett.* **125**, 077701 (2020).
- [24] P. Scarlino, D. J. van Woerkom, A. Stockklauser, J. V. Koski, M. C. Collodo, S. Gasparinetti, C. Reichl, W. Wegscheider, T. Ihn, K. Ensslin, and A. Wallraff, All-Microwave Control and Dispersive Readout of Gate-Defined Quantum Dot Qubits in Circuit Quantum Electrodynamics, *Phys. Rev. Lett.* **122**, 206802 (2019).

- [25] M.-B. Chen, B.-C. Wang, S. Kohler, Y. Kang, T. Lin, S.-S. Gu, H.-O. Li, G.-C. Guo, X. Hu, H.-W. Jiang, G. Cao, and G.-P. Guo, Floquet state depletion in ac-driven circuit QED, *Phys. Rev. B* **103**, 205428 (2021).
- [26] M. Benito and G. Burkard, Hybrid superconductor-semiconductor systems for quantum technology, *Appl. Phys. Lett.* **116**, 190502 (2020).
- [27] M. Russ, C. G. Péterfalvi, and G. Burkard, Theory of valley-resolved spectroscopy of a Si triple quantum dot coupled to a microwave resonator, *J. Phys.: Condens. Matter* **32**, 165301 (2020).
- [28] J. Mielke, J. R. Petta, and G. Burkard, Nuclear spin readout in a cavity-coupled hybrid quantum dot-donor system, *PRX Quantum* **2**, 020347 (2021).
- [29] B. D'Anjou and G. Burkard, Optimal dispersive readout of a spin qubit with a microwave resonator, *Phys. Rev. B* **100**, 245427 (2019).
- [30] G. Engelhardt and J. Cao, Dynamical Symmetries and Symmetry-Protected Selection Rules in Periodically Driven Quantum Systems, *Phys. Rev. Lett.* **126**, 090601 (2021).
- [31] M. Trif and P. Simon, Braiding of Majorana Fermions in a Cavity, *Phys. Rev. Lett.* **122**, 236803 (2019).
- [32] V. L. Grigoryan and K. Xia, Torque-induced dispersive readout in a weakly coupled hybrid system, *Phys. Rev. B* **102**, 064426 (2020).
- [33] B. D'Anjou, Generalized figure of merit for qubit readout, *Phys. Rev. A* **103**, 042404 (2021).
- [34] E. R. Eisenach, J. F. Barry, M. F. O'Keefe, J. M. Schloss, M. H. Steinecker, D. R. Englund, and D. A. Braje, Cavity-enhanced microwave readout of a solid-state spin sensor, *Nat. Commun.* **12**, 1357 (2021).
- [35] J. Ebel, T. Joas, M. Schalk, P. Weinbrenner, A. Angerer, J. Majer, and F. Reinhard, Dispersive readout of room-temperature ensemble spin sensors, *Quantum Sci. Technol.* **6**, 03LT01 (2021).
- [36] M. Benito, X. Mi, J. M. Taylor, J. R. Petta, and G. Burkard, Input-output theory for spin-photon coupling in Si double quantum dots, *Phys. Rev. B* **96**, 235434 (2017).
- [37] G. Burkard and J. R. Petta, Dispersive readout of valley splittings in cavity-coupled silicon quantum dots, *Phys. Rev. B* **94**, 195305 (2016).
- [38] L. Magazzù, P. Forn-Díaz, and M. Grifoni, Transmission spectra of the driven, dissipative Rabi model in the ultrastrong-coupling regime, *Phys. Rev. A* **104**, 053711 (2021).
- [39] D. Zueco, G. M. Reuther, S. Kohler, and P. Hänggi, Qubit-oscillator dynamics in the dispersive regime: Analytical theory beyond the rotating-wave approximation, *Phys. Rev. A* **80**, 033846 (2009).
- [40] X. Mi, J. V. Cady, D. M. Zajac, P. W. Deelman, and J. R. Petta, Strong coupling of a single electron in silicon to a microwave photon, *Science* **355**, 156 (2017).
- [41] E. Kawakami, P. Scarlino, D. R. Ward, F. R. Braakman, D. E. Savage, M. G. Lagally, M. Friesen, S. N. Coppersmith, M. A. Eriksson, and L. M. K. Vandersypen, Electrical control of a long-lived spin qubit in a Si/SiGe quantum dot, *Nat. Nanotechnol.* **9**, 666 (2014).
- [42] D. M. Zajac, T. M. Hazard, X. Mi, E. Nielsen, and J. R. Petta, Scalable Gate Architecture for a One-Dimensional Array of Semiconductor Spin Qubits, *Phys. Rev. Appl.* **6**, 054013 (2016).
- [43] K. Takeda, J. Kamioka, T. Otsuka, J. Yoneda, T. Nakajima, M. R. Delbecq, S. Amaha, G. Allison, T. Kodera, S. Oda, and S. Tarucha, A fault-tolerant addressable spin qubit in a natural silicon quantum dot, *Sci. Adv.* **2**, e1600694 (2016).
- [44] T. Niemczyk, F. Deppe, H. Huebl, E. P. Menzel, F. Hocke, M. J. Schwarz, J. J. García-Ripoll, D. Zueco, T. Hümmer, E. Solano, A. Marx, and R. Gross, Circuit quantum electrodynamics in the ultrastrong-coupling regime, *Nat. Phys.* **6**, 772 (2010).
- [45] P. Forn-Díaz, J. Lisenfeld, D. Marcos, J. J. García-Ripoll, E. Solano, C. J. P. M. Harmans, and J. E. Mooij, Observation of the Bloch-Siegert Shift in a Qubit-Oscillator System in the Ultrastrong Coupling Regime, *Phys. Rev. Lett.* **105**, 237001 (2010).
- [46] P. Forn-Díaz, J. J. García-Ripoll, B. Peropadre, J. L. Orgiazzi, M. A. Yurtalan, R. Belyansky, C. M. Wilson, and A. Lupascu, Ultrastrong coupling of a single artificial atom to an electromagnetic continuum in the nonperturbative regime, *Nat. Phys.* **13**, 39 (2017).
- [47] Z. Chen, Y. Wang, T. Li, L. Tian, Y. Qiu, K. Inomata, F. Yoshihara, S. Han, F. Nori, J. S. Tsai, and J. Q. You, Single-photon-driven high-order sideband transitions in an ultrastrongly coupled circuit-quantum-electrodynamics system, *Phys. Rev. A* **96**, 012325 (2017).
- [48] F. Yoshihara, T. Fuse, S. Ashhab, K. Kakuyanagi, S. Saito, and K. Semba, Superconducting qubit-oscillator circuit beyond the ultrastrong-coupling regime, *Nat. Phys.* **13**, 44 (2017).
- [49] A. M. Sokolov and E. V. Stolyarov, Single-photon limit of dispersive readout of a qubit with a photodetector, *Phys. Rev. A* **101**, 042306 (2020).
- [50] M. Brune, S. Haroche, V. Lefevre, J. M. Raimond, and N. Zagury, Quantum Nondemolition Measurement of Small Photon Numbers by Rydberg-Atom Phase-Sensitive Detection, *Phys. Rev. Lett.* **65**, 976 (1990).
- [51] M. Brune, P. Nussenzweig, F. Schmidt-Kaler, F. Bernardot, A. Maali, J. M. Raimond, and S. Haroche, From Lamb Shift to Light Shifts: Vacuum and Subphoton Cavity Fields Measured by Atomic Phase Sensitive Detection, *Phys. Rev. Lett.* **72**, 3339 (1994).
- [52] S. Gleyzes, S. Kuhr, C. Guerlin, J. Bernu, S. Deléglise, U. B. Hoff, M. Brune, J. M. Raimond, and S. Haroche, Quantum jumps of light recording the birth and death of a photon in a cavity, *Nature (London)* **446**, 297 (2007).
- [53] M. Aspelmeyer, T. J. Kippenberg, and F. Marquardt, Cavity optomechanics, *Rev. Mod. Phys.* **86**, 1391 (2014).
- [54] J. D. Thompson, B. M. Zwickl, A. M. Jayich, F. Marquardt, S. M. Girvin, and J. G. E. Harris, Strong dispersive coupling of a high-finesse cavity to a micromechanical membrane, *Nature (London)* **452**, 72 (2008).
- [55] C. A. Regal, J. D. Teufel, and K. W. Lehnert, Measuring nanomechanical motion with a microwave cavity interferometer, *Nat. Phys.* **4**, 555 (2008).
- [56] A. Wallraff, D. I. Schuster, A. Blais, L. Frunzio, J. Majer, M. H. Devoret, S. M. Girvin, and R. J. Schoelkopf, Approaching Unit Visibility for Control of a Superconducting Qubit with Dispersive Readout, *Phys. Rev. Lett.* **95**, 060501 (2005).
- [57] D. I. Schuster, A. Wallraff, A. Blais, L. Frunzio, R. S. Huang, J. Majer, S. M. Girvin, and R. J. Schoelkopf, ac Stark Shift and Dephasing of a Superconducting Qubit Strongly

- Coupled to a Cavity Field, *Phys. Rev. Lett.* **94**, 123602 (2005).
- [58] J. Majer, J. M. Chow, J. M. Gambetta, J. Koch, B. R. Johnson, J. A. Schreier, L. Frunzio, D. I. Schuster, A. A. Houck, A. Wallraff, A. Blais, M. H. Devoret, S. M. Girvin, and R. J. Schoelkopf, Coupling superconducting qubits via a cavity bus, *Nature (London)* **449**, 443 (2007).
- [59] T. D. Ladd, F. Jelezko, R. Laflamme, Y. Nakamura, C. Monroe, and J. L. O'Brien, Quantum computers, *Nature (London)* **464**, 45 (2010).
- [60] H. P. Breuer and F. Petruccione, *The Theory of Open Quantum Systems* (Oxford University Press, Oxford, 2002).
- [61] U. Weiss, *Quantum Dissipative Systems* (World Scientific, Singapore, 2008).
- [62] J.-G. Li, J. Zou, and B. Shao, Non-Markovianity of the damped Jaynes-Cummings model with detuning, *Phys. Rev. A* **81**, 062124 (2010).
- [63] C. W. Gardiner and P. Zoller, *Quantum Noise* (Springer, Berlin, 2000).
- [64] R. Lo Franco, B. Bellomo, S. Maniscalco, and G. Compagno, Dynamics of quantum correlations in two-qubit systems within non-Markovian environments, *Int. J. Mod. Phys. B* **27**, 1345053 (2013).
- [65] F. Caruso, V. Giovannetti, C. Lupo, and S. Mancini, Quantum channels and memory effects, *Rev. Mod. Phys.* **86**, 1203 (2014).
- [66] M. J. Hartmann, F. G. S. L. Brandão, and M. B. Plenio, Strongly interacting polaritons in coupled arrays of cavities, *Nat. Phys.* **2**, 849 (2006).
- [67] T. Pellizzari, Quantum Networking with Optical Fibres, *Phys. Rev. Lett.* **79**, 5242 (1997).
- [68] A. Biswas and D. A. Lidar, Robust transmission of non-Gaussian entanglement over optical fibers, *Phys. Rev. A* **74**, 062303 (2006).
- [69] Q. A. Turchette, C. J. Myatt, B. E. King, C. A. Sackett, D. Kielpinski, W. M. Itano, C. Monroe, and D. J. Wineland, Decoherence and decay of motional quantum states of a trapped atom coupled to engineered reservoirs, *Phys. Rev. A* **62**, 053807 (2000).
- [70] C. J. Myatt, B. E. King, Q. A. Turchette, C. A. Sackett, D. Kielpinski, W. M. Itano, C. Monroe, and D. J. Wineland, Decoherence of quantum superpositions through coupling to engineered reservoirs, *Nature (London)* **403**, 269 (2000).
- [71] S. Maniscalco, J. Piilo, F. Intravaia, F. Petruccione, and A. Messina, Simulating quantum Brownian motion with single trapped ions, *Phys. Rev. A* **69**, 052101 (2004).
- [72] M. Bayindir, B. Temelkuran, and E. Ozbay, Tight-Binding Description of the Coupled Defect Modes in Three-Dimensional Photonic Crystals, *Phys. Rev. Lett.* **84**, 2140 (2000).
- [73] N. Stefanou and A. Modinos, Impurity bands in photonic insulators, *Phys. Rev. B* **57**, 12127 (1998).
- [74] Y. Xu, Y. Li, R. K. Lee, and A. Yariv, Scattering-theory analysis of waveguide-resonator coupling, *Phys. Rev. E* **62**, 7389 (2000).
- [75] L.-L. Lin, Z.-Y. Li, and B. Lin, Engineering waveguide-cavity resonant side coupling in a dynamically tunable ultracompact photonic crystal filter, *Phys. Rev. B* **72**, 165330 (2005).
- [76] K. W. Chang and C. K. Law, Non-Markovian master equation for a damped oscillator with time-varying parameters, *Phys. Rev. A* **81**, 052105 (2010).
- [77] H.-T. Tan and W.-M. Zhang, Non-Markovian dynamics of an open quantum system with initial system-reservoir correlations: A nanocavity coupled to a coupled-resonator optical waveguide, *Phys. Rev. A* **83**, 032102 (2011).
- [78] S. Longhi, Non-Markovian decay and lasing condition in an optical microcavity coupled to a structured reservoir, *Phys. Rev. A* **74**, 063826 (2006).
- [79] I. de Vega and D. Alonso, Dynamics of non-Markovian open quantum systems, *Rev. Mod. Phys.* **89**, 015001 (2017).
- [80] A. J. Leggett, S. Chakravarty, A. T. Dorsey, M. P. A. Fisher, A. Garg, and W. Zwerger, Dynamics of the dissipative two-state system, *Rev. Mod. Phys.* **59**, 1 (1987).
- [81] S. Gröblacher, A. Trubarov, N. Prigge, G. D. Cole, M. Aspelmeyer, and J. Eisert, Observation of non-Markovian micromechanical Brownian motion, *Nat. Commun.* **6**, 7606 (2015).
- [82] A. D'Arrigo, R. Lo Franco, G. Benenti, E. Paladino, and G. Falci, Recovering entanglement by local operations, *Ann. Phys. (NY)* **350**, 211 (2014).
- [83] R. Lo Franco, A. D'Arrigo, G. Falci, G. Compagno, and E. Paladino, Preserving entanglement and nonlocality in solid-state qubits by dynamical decoupling, *Phys. Rev. B* **90**, 054304 (2014).
- [84] B. Bylicka, D. Chruściński, and S. Maniscalco, Non-Markovianity and reservoir memory of quantum channels: A quantum information theory perspective, *Sci. Rep.* **4**, 5720 (2014).
- [85] S.-B. Xue, R.-B. Wu, W.-M. Zhang, J. Zhang, C.-W. Li, and T.-J. Tarn, Decoherence suppression via non-Markovian coherent feedback control, *Phys. Rev. A* **86**, 052304 (2012).
- [86] H. P. Breuer, E. M. Laine, J. Piilo, and B. Vacchini, Colloquium: Non-Markovian dynamics in open quantum systems, *Rev. Mod. Phys.* **88**, 021002 (2016).
- [87] H. P. Breuer, E. M. Laine, and J. Piilo, Measure for the Degree of Non-Markovian Behavior of Quantum Processes in Open Systems, *Phys. Rev. Lett.* **103**, 210401 (2009).
- [88] E. M. Laine, J. Piilo, and H. P. Breuer, Measure for the non-Markovianity of quantum processes, *Phys. Rev. A* **81**, 062115 (2010).
- [89] C. Addis, B. Bylicka, D. Chruściński, and S. Maniscalco, Comparative study of non-Markovianity measures in exactly solvable one- and two-qubit models, *Phys. Rev. A* **90**, 052103 (2014).
- [90] S. Wißmann, A. Karlsson, E. M. Laine, J. Piilo, and H. P. Breuer, Optimal state pairs for non-Markovian quantum dynamics, *Phys. Rev. A* **86**, 062108 (2012).
- [91] S. Wißmann, H.-P. Breuer, and B. Vacchini, Generalized trace-distance measure connecting quantum and classical non-Markovianity, *Phys. Rev. A* **92**, 042108 (2015).
- [92] H. Z. Shen, D. X. Li, S.-L. Su, Y. H. Zhou, and X. X. Yi, Exact non-Markovian dynamics of qubits coupled to two interacting environments, *Phys. Rev. A* **96**, 033805 (2017); H. Z. Shen, S. L. Su, Y. H. Zhou, and X. X. Yi, Non-Markovian quantum Brownian motion in one dimension in electric fields, *ibid.* **97**, 042121 (2018).
- [93] S. Lorenzo, F. Plastina, and M. Paternostro, Geometrical characterization of non-Markovianity, *Phys. Rev. A* **88**, 020102(R) (2013).

- [94] Á. Rivas, S. F. Huelga, and M. B. Plenio, Entanglement and Non-Markovianity of Quantum Evolutions, *Phys. Rev. Lett.* **105**, 050403 (2010).
- [95] S. Luo, S. Fu, and H. Song, Quantifying non-Markovianity via correlations, *Phys. Rev. A* **86**, 044101 (2012).
- [96] M. M. Wolf, J. Eisert, T. S. Cubitt, and J. I. Cirac, Assessing Non-Markovian Quantum Dynamics, *Phys. Rev. Lett.* **101**, 150402 (2008).
- [97] X.-M. Lu, X. Wang, and C. P. Sun, Quantum Fisher information flow and non-Markovian processes of open systems, *Phys. Rev. A* **82**, 042103 (2010).
- [98] D. Chruściński and S. Maniscalco, Degree of Non-Markovianity of Quantum Evolution, *Phys. Rev. Lett.* **112**, 120404 (2014).
- [99] M. J. Collett and C. W. Gardiner, Squeezing of intracavity and traveling-wave light fields produced in parametric amplification, *Phys. Rev. A* **30**, 1386 (1984).
- [100] C. W. Gardiner and M. J. Collett, Input and output in damped quantum systems: Quantum stochastic differential equations and the master equation, *Phys. Rev. A* **31**, 3761 (1985).
- [101] L. Diósi, Non-Markovian open quantum systems: Input-output fields, memory, and monitoring, *Phys. Rev. A* **85**, 034101 (2012).
- [102] H. Z. Shen, M. Qin, and X. X. Yi, Single-photon storing in coupled non-Markovian atom-cavity system, *Phys. Rev. A* **88**, 033835 (2013).
- [103] J. Zhang, Y.-x. Liu, R.-B. Wu, K. Jacobs, and F. Nori, Non-Markovian quantum input-output networks, *Phys. Rev. A* **87**, 032117 (2013).
- [104] H.-N. Xiong, W.-M. Zhang, M. W.-Y. Tu, and D. Braun, Dynamically stabilized decoherence-free states in non-Markovian open fermionic systems, *Phys. Rev. A* **86**, 032107 (2012).
- [105] H. Z. Shen, D. X. Li, and X. X. Yi, Non-Markovian linear response theory for quantum open systems and its applications, *Phys. Rev. E* **95**, 012156 (2017).
- [106] P. Haikka and S. Maniscalco, Non-Markovian dynamics of a damped driven two-state system, *Phys. Rev. A* **81**, 052103 (2010).
- [107] G. E. Uhlenbeck and L. S. Ornstein, On the theory of the Brownian motion, *Phys. Rev.* **36**, 823 (1930).
- [108] D. T. Gillespie, Exact numerical simulation of the Ornstein-Uhlenbeck process and its integral, *Phys. Rev. E* **54**, 2084 (1996).
- [109] J. Jing and T. Yu, Non-Markovian Relaxation of a Three-Level System: Quantum Trajectory Approach, *Phys. Rev. Lett.* **105**, 240403 (2010).
- [110] D. F. Walls and G. J. Milburn, *Quantum Optics* (Springer, Berlin, 1994).
- [111] M. O. Scully and M. S. Zubairy, *Quantum Optics* (Cambridge University Press, Cambridge, 1997).
- [112] C. Uchiyama, M. Aihara, M. Saeki, and S. Miyashita, Master equation approach to line shape in dissipative systems, *Phys. Rev. E* **80**, 021128 (2009).
- [113] M. Saeki, C. Uchiyama, T. Mori, and S. Miyashita, Comparison among various expressions of complex admittance for quantum systems in contact with a heat reservoir, *Phys. Rev. E* **81**, 031131 (2010).
- [114] H. Z. Shen, M. Qin, X. Q. Shao, and X. X. Yi, General response formula and application to topological insulator in quantum open system, *Phys. Rev. E* **92**, 052122 (2015).
- [115] K. D. Petersson, L. W. McFaul, M. D. Schroer, M. Jung, J. M. Taylor, A. A. Houck, and J. R. Petta, Circuit quantum electrodynamics with a spin qubit, *Nature (London)* **490**, 380 (2012).
- [116] X. Mi, M. Benito, S. Putz, D. M. Zajac, J. M. Taylor, G. Burkard, and J. R. Petta, A coherent spin-photon interface in silicon, *Nature (London)* **555**, 599 (2018).
- [117] N. Samkharadze, G. Zheng, N. Kalhor, D. Brousse, A. Sammak, U. C. Mendes, A. Blais, G. Scappucci, and L. M. K. Vandersypen, Strong spin-photon coupling in silicon, *Science* **359**, 1123 (2018).
- [118] R. J. Thompson, G. Rempe, and H. J. Kimble, Observation of Normal-Mode Splitting for an Atom in an Optical Cavity, *Phys. Rev. Lett.* **68**, 1132 (1992).
- [119] S. J. van Enk, J. I. Cirac, and P. Zoller, Photonic Channels for Quantum Communication, *Science* **279**, 205 (1998).
- [120] S. Kohler, J. Lehmann, and P. Hänggi, Driven quantum transport on the nanoscale, *Phys. Rep.* **406**, 379 (2005).
- [121] S. Kohler, T. Dittrich, and P. Hänggi, Floquet-Markovian description of the parametrically driven, dissipative harmonic quantum oscillator, *Phys. Rev. E* **55**, 300 (1997).
- [122] H. Sambe, Steady states and quasienergies of a quantum-mechanical system in an oscillating field, *Phys. Rev. A* **7**, 2203 (1973).
- [123] J. H. Shirley, Solution of the Schrödinger equation with a Hamiltonian periodic in time, *Phys. Rev.* **138**, B979 (1965).
- [124] A. Eckardt, Colloquium: Atomic quantum gases in periodically driven optical lattices, *Rev. Mod. Phys.* **89**, 011004 (2017).
- [125] A. Eckardt and E. Anisimovas, High-frequency approximation for periodically driven quantum systems from a Floquet-space perspective, *New J. Phys.* **17**, 093039 (2015).
- [126] C. Chen, J.-H. An, H.-G. Luo, C. P. Sun, and C. H. Oh, Floquet control of quantum dissipation in spin chains, *Phys. Rev. A* **91**, 052122 (2015).
- [127] A. Verdeny, A. Mielke, and F. Mintert, Accurate Effective Hamiltonians via Unitary Flow in Floquet Space, *Phys. Rev. Lett.* **111**, 175301 (2013).
- [128] J. I. Cirac, P. Zoller, H. J. Kimble, and H. Mabuchi, Quantum State Transfer and Entanglement Distribution among Distant Nodes in a Quantum Network, *Phys. Rev. Lett.* **78**, 3221 (1997).
- [129] S. J. van Enk, J. I. Cirac, and P. Zoller, Ideal Quantum Communication over Noisy Channels: A Quantum Optical Implementation, *Phys. Rev. Lett.* **78**, 4293 (1997).
- [130] S. Clark, A. Peng, M. Gu, and S. Parkins, Unconditional Preparation of Entanglement between Atoms in Cascaded Optical Cavities, *Phys. Rev. Lett.* **91**, 177901 (2003).
- [131] W. Yao, R.-B. Liu, and L. J. Sham, Theory of control of the dynamics of the interface between stationary and flying qubits, *J. Opt. B* **7**, S318 (2005).
- [132] F.-Y. Hong and S.-J. Xiong, Quantum communication in a network with serious imperfections, *Phys. Rev. A* **76**, 052302 (2007).
- [133] F. Motzoi, L. Buchmann, and C. Dickel, Simple, smooth and fast pulses for dispersive measurements in cavities and quantum networks, [arXiv:1809.04116](https://arxiv.org/abs/1809.04116).

- [134] C. A. Cain and C. H. Wu, Quantum network theory of computing with respect to entangled flux qubits and external perturbation, *J. Appl. Phys.* **113**, 154309 (2013).
- [135] J. Nokkala, R. Martínez-Peña, R. Zambrini, and M. C. Soriano, High-performance reservoir computing with fluctuations in linear networks, *IEEE Trans. Neural Netw. Learn. Syst.* (unpublished).
- [136] R. Huang, X. Tan, and Q. Xu, Variational quantum tensor networks classifiers, *Neurocomputing* **452**, 89 (2021).
- [137] E. Farhi and H. Neven, Classification with quantum neural networks on near term processors, [arXiv:1802.06002](https://arxiv.org/abs/1802.06002).
- [138] C. Dickel, J. J. Wesdorp, N. K. Langford, S. Peiter, R. Sagastizabal, A. Bruno, B. Criger, F. Motzoi, and L. DiCarlo, Chip-to-chip entanglement of transmon qubits using engineered measurement fields, *Phys. Rev. B* **97**, 064508 (2018).
- [139] S. Felicetti, M. Sanz, L. Lamata, G. Romero, G. Johansson, P. Delsing, and E. Solano, Dynamical Casimir Effect Entangles Artificial Atoms, *Phys. Rev. Lett.* **113**, 093602 (2014).
- [140] B. Abdo, A. Kamal, and M. Devoret, Nondegenerate three-wave mixing with the Josephson ring modulator, *Phys. Rev. B* **87**, 014508 (2013).
- [141] H. Z. Shen, C. Shang, Y. H. Zhou, and X. X. Yi, Unconventional single-photon blockade in non-Markovian systems, *Phys. Rev. A* **98**, 023856 (2018); H. Z. Shen, Q. Wang, J. Wang, and X. X. Yi, Nonreciprocal unconventional photon blockade in a driven dissipative cavity with parametric amplification, *ibid.* **101**, 013826 (2020).
- [142] F. Mivehvar, F. Piazza, T. Donner, and H. Ritsch, Cavity QED with quantum gases: New paradigms in many-body physics, *Adv. Phys.* **70**, 1 (2021).
- [143] A. H. Safavi-Naeini, J. T. Hill, S. Meenehan, J. Chan, S. Gröblacher, and O. Painter, Two-Dimensional Phononic-Photonic Band Gap Optomechanical Crystal Cavity, *Phys. Rev. Lett.* **112**, 153603 (2014).
- [144] T. K. Paraíso, M. Kalae, L. Zang, H. Pfeifer, F. Marquardt, and O. Painter, Position-Squared Coupling in a Tunable Photonic Crystal Optomechanical Cavity, *Phys. Rev. X* **5**, 041024 (2015).
- [145] E. Kim, X. Zhang, V. S. Ferreira, J. Banker, J. K. Iverson, A. Sipahigil, M. Bello, A. González-Tudela, M. Mirhosseini, and O. Painter, Quantum Electrodynamics in a Topological Waveguide, *Phys. Rev. X* **11**, 011015 (2021).
- [146] J. P. Covey, A. Sipahigil, S. Szoke, N. Sinclair, M. Endres, and O. Painter, Telecom-Band Quantum Optics with Ytterbium Atoms and Silicon Nanophotonics, *Phys. Rev. Appl.* **11**, 034044 (2019).
- [147] V. S. Ferreira, J. Banker, A. Sipahigil, M. H. Matheny, A. J. Keller, E. Kim, M. Mirhosseini, and O. Painter, Collapse and Revival of an Artificial Atom Coupled to a Structured Photonic Reservoir, *Phys. Rev. X* **11**, 041043 (2021).
- [148] S. M. Meenehan, J. D. Cohen, G. S. MacCabe, F. Marsili, M. D. Shaw, and O. Painter, Pulsed Excitation Dynamics of an Optomechanical Crystal Resonator near Its Quantum Ground State of Motion, *Phys. Rev. X* **5**, 041002 (2015).
- [149] H. Ren, M. H. Matheny, G. S. MacCabe, J. Luo, H. Pfeifer, M. Mirhosseini, and O. Painter, Two-dimensional optomechanical crystal cavity with high quantum cooperativity, *Nat. Commun.* **11**, 3373 (2020).
- [150] M. Kalae, M. Mirhosseini, P. B. Dieterle, M. Peruzzo, J. M. Fink, and O. Painter, Quantum electromechanics of a hypersonic crystal, *Nat. Nanotechnol.* **14**, 334 (2019).
- [151] M. Mirhosseini, E. Kim, V. S. Ferreira, M. Kalae, A. Sipahigil, A. J. Keller, and O. Painter, Superconducting metamaterials for waveguide quantum electrodynamics, *Nat. Commun.* **9**, 3706 (2018).
- [152] K. Fang, M. H. Matheny, X. Luan, and O. Painter, Optical transduction and routing of microwave phonons in cavity-optomechanical circuits, *Nat. Photon.* **10**, 489 (2016).
- [153] S.-P. Yu, J. D. Hood, J. A. Muniz, M. J. Martin, R. Norte, C.-L. Hung, S. M. Meenehan, J. D. Cohen, O. Painter, and H. J. Kimble, Nanowire photonic crystal waveguides for single-atom trapping and strong light-matter interactions, *Appl. Phys. Lett.* **104**, 111103 (2014).
- [154] M. Eichenfield, J. Chan, R. M. Camacho, K. J. Vahala, and O. Painter, Optomechanical crystals, *Nature (London)* **462**, 78 (2009).
- [155] M. Eichenfield, R. Camacho, J. Chan, K. J. Vahala, and O. Painter, A picogram- and nanometre-scale photonic-crystal optomechanical cavity, *Nature (London)* **459**, 550 (2009).
- [156] B.-H. Liu, L. Li, Y.-F. Huang, C.-F. Li, G.-C. Guo, E.-M. Laine, H.-P. Breuer, and J. Piilo, Experimental control of the transition from Markovian to non-Markovian dynamics of open quantum systems, *Nat. Phys.* **7**, 931 (2011).
- [157] U. Hoeppe, C. Wolff, J. Küchenmeister, J. Niegemann, M. Drescher, H. Benner, and K. Busch, Direct Observation of Non-Markovian Radiation Dynamics in 3D Bulk Photonic Crystals, *Phys. Rev. Lett.* **108**, 043603 (2012).
- [158] J.-S. Xu, X.-Y. Xu, C.-F. Li, C.-J. Zhang, X.-B. Zou, and G.-C. Guo, Experimental investigation of classical and quantum correlations under decoherence, *Nat. Commun.* **1**, 7 (2010).
- [159] J.-S. Xu, C.-F. Li, C.-J. Zhang, X.-Y. Xu, Y.-S. Zhang, and G.-C. Guo, Experimental investigation of the non-Markovian dynamics of classical and quantum correlations, *Phys. Rev. A* **82**, 042328 (2010).
- [160] K. H. Madsen, S. Ates, T. Lund-Hansen, A. Löffler, S. Reitzenstein, A. Forchel, and P. Lodahl, Observation of Non-Markovian Dynamics of a Single Quantum Dot in a Micropillar Cavity, *Phys. Rev. Lett.* **106**, 233601 (2011).
- [161] A. Orioux, A. D'Arrigo, G. Ferranti, R. Lo Franco, G. Benenti, E. Paladino, G. Falci, F. Sciarrino, and P. Mataloni, Experimental on-demand recovery of entanglement by local operations within non-Markovian dynamics, *Sci. Rep.* **5**, 8575 (2015).
- [162] M. W. Jack and J. J. Hope, Resonance fluorescence in a band-gap material: Direct numerical simulation of non-Markovian evolution, *Phys. Rev. A* **63**, 043803 (2001).
- [163] S. M. Barnett and P. M. Radmore, *Methods in Theoretical Quantum Optics* (Oxford University Press, Oxford, 1997).
- [164] B. M. Garraway, Nonperturbative decay of an atomic system in a cavity, *Phys. Rev. A* **55**, 2290 (1997).
- [165] B. M. Garraway, Decay of an atom coupled strongly to a reservoir, *Phys. Rev. A* **55**, 4636 (1997).

- [166] Z.-X. Man, N. B. An, and Y.-J. Xia, Non-Markovianity of a two-level system transversally coupled to multiple bosonic reservoirs, *Phys. Rev. A* **90**, 062104 (2014).
- [167] Z.-X. Man, N.-B. An, and Y.-J. Xia, Non-Markovian dynamics of a two-level system in the presence of hierarchical environments, *Opt. Express* **23**, 5763 (2015).
- [168] L. Mazzola, S. Maniscalco, J. Piilo, K. A. Suominen, and B. M. Garraway, Pseudomodes as an effective description of memory: Non-Markovian dynamics of two-state systems in structured reservoirs, *Phys. Rev. A* **80**, 012104 (2009).
- [169] G. Pleasance and B. M. Garraway, Application of quantum Darwinism to a structured environment, *Phys. Rev. A* **96**, 062105 (2017).
- [170] C. T. Hann, S. S. Elder, C. S. Wang, K. Chou, R. J. Schoelkopf, and L. Jiang, Robust readout of bosonic qubits in the dispersive coupling regime, *Phys. Rev. A* **98**, 022305 (2018).
- [171] T. Walter, P. Kurpiers, S. Gasparinetti, P. Magnard, A. Potočnik, Y. Salathé, M. Pechal, M. Mondal, M. Oppliger, C. Eichler, and A. Wallraff, Rapid High-Fidelity Single-Shot Dispersive Readout of Superconducting Qubits, *Phys. Rev. Appl.* **7**, 054020 (2017).
- [172] P. M. Billangeon, J. S. Tsai, and Y. Nakamura, Circuit-QED-based scalable architectures for quantum information processing with superconducting qubits, *Phys. Rev. B* **91**, 094517 (2015).
- [173] Y. Salathé, P. Kurpiers, T. Karg, C. Lang, C. K. Andersen, A. Akin, S. Krinner, C. Eichler, and A. Wallraff, Low-Latency Digital Signal Processing for Feedback and Feedforward in Quantum Computing and Communication, *Phys. Rev. Appl.* **9**, 034011 (2018).
- [174] S. K. Manikandan, C. Elouard, and A. N. Jordan, Fluctuation theorems for continuous quantum measurements and absolute irreversibility, *Phys. Rev. A* **99**, 022117 (2019).
- [175] U. Vool, S. Shankar, S. O. Mundhada, N. Ofek, A. Narla, K. Sliwa, E. Zolys-Geller, Y. Liu, L. Frunzio, R. J. Schoelkopf, S. M. Girvin, and M. H. Devoret, Continuous Quantum Non-demolition Measurement of the Transverse Component of a Qubit, *Phys. Rev. Lett.* **117**, 133601 (2016).
- [176] T. Peronnin, D. Marković, Q. Ficheux, and B. Huard, Sequential Dispersive Measurement of a Superconducting Qubit, *Phys. Rev. Lett.* **124**, 180502 (2020).
- [177] H. Grabert and M. Thorwart, Quantum mechanical response to a driven Caldeira-Leggett bath, *Phys. Rev. E* **98**, 012122 (2018).
- [178] A. Shabani, J. Roden, and K. B. Whaley, Continuous Measurement of a Non-Markovian Open Quantum System, *Phys. Rev. Lett.* **112**, 113601 (2014).
- [179] L.-P. Yang, C. Y. Cai, D. Z. Xu, W.-M. Zhang, and C. P. Sun, Master equation and dispersive probing of a non-Markovian process, *Phys. Rev. A* **87**, 012110 (2013).
- [180] G. M. Reuther, P. Hänggi, and S. Kohler, Non-Markovian qubit decoherence during dispersive readout, *Phys. Rev. A* **85**, 062123 (2012).
- [181] H. Z. Shen, S. Xu, H. T. Cui, and X. X. Yi, Non-Markovian dynamics of a system of two-level atoms coupled to a structured environment, *Phys. Rev. A* **99**, 032101 (2019); H. Z. Shen, X. Q. Shao, G. C. Wang, X. L. Zhao, and X. X. Yi, Quantum phase transition in a coupled two-level system embedded in anisotropic three-dimensional photonic crystals, *Phys. Rev. E* **93**, 012107 (2016).
- [182] H. Z. Shen, S. Xu, S. Yi, and X. X. Yi, Controllable dissipation of a qubit coupled to an engineering reservoir, *Phys. Rev. A* **98**, 062106 (2018).
- [183] T. Shi, Y. H. Wu, A. González-Tudela, and J. I. Cirac, Bound States in Boson Impurity Models, *Phys. Rev. X* **6**, 021027 (2016).
- [184] T. Shi, Y.-H. Wu, A. González-Tudela, and J. I. Cirac, Effective many-body Hamiltonians of qubit-photon bound states, *New J. Phys.* **20**, 105005 (2018).
- [185] G. Calajó and P. Rabl, Strong coupling between moving atoms and slow-light Cherenkov photons, *Phys. Rev. A* **95**, 043824 (2017).
- [186] J. V. Koski, A. J. Landig, A. Pályi, P. Scarlino, C. Reichl, W. Wegscheider, G. Burkard, A. Wallraff, K. Ensslin, and T. Ihn, Floquet Spectroscopy of a Strongly Driven Quantum Dot Charge Qubit with a Microwave Resonator, *Phys. Rev. Lett.* **121**, 043603 (2018).
- [187] T. Shi, Y. Chang, and J. J. García-Ripoll, Ultrastrong Coupling Few-Photon Scattering Theory, *Phys. Rev. Lett.* **120**, 153602 (2018).
- [188] L. Lo and C. K. Law, Quantum radiation from a shaken two-level atom in vacuum, *Phys. Rev. A* **98**, 063807 (2018).
- [189] W.-Z. Zhang, J. Cheng, W.-D. Li, and L. Zhou, Optomechanical cooling in the non-Markovian regime, *Phys. Rev. A* **93**, 063853 (2016).
- [190] W.-Z. Zhang, Y. Han, B. Xiong, and L. Zhou, Optomechanical force sensor in non-Markovian regime, *New J. Phys.* **19**, 083022 (2017).
- [191] J. F. Triana, A. F. Estrada, and L. A. Pachón, Ultrafast Optimal Sideband Cooling under Non-Markovian Evolution, *Phys. Rev. Lett.* **116**, 183602 (2016).
- [192] J. C. Sankey, C. Yang, B. M. Zwickl, A. M. Jayich, and J. G. E. Harris, Strong and tunable nonlinear optomechanical coupling in a low-loss system, *Nat. Phys.* **6**, 707 (2010).
- [193] M. Bhattacharya, H. Uys, and P. Meystre, Optomechanical trapping and cooling of partially reflective mirrors, *Phys. Rev. A* **77**, 033819 (2008).
- [194] J.-Q. Liao and F. Nori, Photon blockade in quadratically coupled optomechanical systems, *Phys. Rev. A* **88**, 023853 (2013).
- [195] H. K. Cheung and C. K. Law, Nonadiabatic optomechanical Hamiltonian of a moving dielectric membrane in a cavity, *Phys. Rev. A* **84**, 023812 (2011).
- [196] W. Zhang, D.-S. Ding, Y.-B. Sheng, L. Zhou, B.-S. Shi, and G.-C. Guo, Quantum Secure Direct Communication with Quantum Memory, *Phys. Rev. Lett.* **118**, 220501 (2017).
- [197] L. Magazzù, P. Forn-Díaz, R. Belyansky, J. L. Orgiazzi, M. A. Yurtalan, M. R. Otto, A. Lupascu, C. M. Wilson, and M. Grifoni, Probing the strongly driven spin-boson model in a superconducting quantum circuit, *Nat. Commun.* **9**, 1403 (2018).
- [198] R. Kubo, Statistical-mechanical theory of irreversible processes. I. General theory and simple applications to magnetic and conduction problems, *J. Phys. Soc. Jpn.* **12**, 570 (1957).
- [199] A. Castro and I. V. Tokatly, Quantum optimal control theory in the linear response formalism, *Phys. Rev. A* **84**, 033410 (2011).
- [200] S. Blanes, F. Casas, J. A. Oteo, and J. Ros, The Magnus expansion and some of its applications, *Phys. Rep.* **470**, 151 (2009).